

On Two Nucleons Near Unitarity with Perturbative Pions

Yu-Ping Teng^{a,b,1}

and

Harald W. Griesshammer^{a,2}

^a *Institute for Nuclear Studies, Department of Physics,
The George Washington University, Washington DC 20052, USA*

^b *Department of Physics, University of Wisconsin-Milwaukee, Milwaukee WI 53211, USA*

Abstract

We explore the expansion of two-nucleon S-wave scattering phase shifts and pole parameters about Unitarity in Chiral Effective Field Theory with Perturbative Pions at next-to-next-to leading order (N²LO): LO contains no scale but the scattering momentum; NLO consists of contributions from scattering length, effective range and non-iterated one-pion exchange (OPE); and N²LO adds only once-iterated OPE. We take advantage of the high degree of symmetry of the nontrivial fixed point at Unitarity, where Physics is universal and invariant under both scaling and Wigner’s combined SU(4) transformation of spin and isospin. Both are explicitly but weakly broken in the Unitarity Expansion, including by pion exchange. This version should apply in the Unitarity Window (phase shifts $45^\circ \lesssim \delta(k) \lesssim 135^\circ$), including around momenta $k \approx m_\pi$. Agreement in the 1S_0 channel is very good. Apparent large discrepancies in the 3S_1 channel even at $k \approx 100$ MeV are remedied by taking only the central part of the pion’s N²LO contribution. In contradistinction to the tensor part, it is invariant under Wigner-SU(4) symmetry and hence identical in 1S_0 and 3S_1 . The pionic part at NLO is Wigner-invariant. In the resulting χ EFT with Perturbative Pions in the Unitarity Expansion, both channels match empirical phase shifts and pole parameters well within several mutually consistent quantitative theory uncertainty estimates. Pionic effects are small, even for $k \gtrsim m_\pi$. Empirically determined breakdown scales are consistent with the scale $\bar{\Lambda}_{\text{NN}} = \frac{16\pi f_\pi^2}{gA^2M} \approx 300$ MeV where iterated OPE is not suppressed. We therefore hypothesise: The footprint of both scale invariance and Wigner symmetry in the Unitarity Expansion shows *persistence*, *i.e.* both dominate even for $k \gtrsim m_\pi$ and are more relevant than chiral symmetry, so that the tensor/Wigner-SU(4) symmetry-breaking part of OPE does not enter before N³LO. We also speculate that this may resolve a conflict with the strength of the tensor interaction in the large- N_C expansion.

Suggested Keywords: Chiral Perturbation Theory, Chiral Effective Field Theory, perturbative pions, Unitarity, universality, scale invariance, Wigner-SU(4) spin-isospin symmetry, chiral symmetry, two-nucleon scattering.

¹Email: yteng@uwm.edu

²Email: hgrie@gwu.edu (corresponding author)

1 Introduction

Why are the observables of few-nucleon systems dominated by anomalous scales? The deuteron is an exceptionally shallow bound state in the 3S_1 channel of NN scattering, with a binding momentum of 45 MeV set by the inverse of the scattering length $a(^3S_1) \approx 5$ fm. Likewise the 1S_0 channel has a virtual bound state at a binding momentum of -7 MeV from $a(^1S_0) \approx -24$ fm. These scales differ much from the natural low-momentum QCD scales of Nuclear Physics, the pion mass $m_\pi \approx 140$ MeV and $\frac{1}{m_\pi} \approx 1.4$ fm. The combined evidence from lattice computations and chiral extrapolations suggest that this fine tuning holds in QCD only in a small window around the physical value of the pion mass [1–3].

Effective Field Theories (EFTs) of Nuclear Physics do not offer an explanation. Rather, they simply impose an ordering scheme whose leading-order (LO) is found by iterating a NN interaction infinitely often. In the version of Chiral Effective Field Theory (χ EFT) which is usually employed (see *e.g.* [4, 5] for recent reviews), this LO iterates one-pion exchange (OPE) and contact terms which are tuned to reproduce the shallow bound states. This is the χ EFT with Nonperturbative Pions. Perfectly valid and consistent versions of χ EFT exist in which LO is perturbative and the binding energy of light nuclei is set by the scale $\frac{m_\pi^2}{M}$ with M the nucleon mass. But these are not realised in Nature.

We will argue that a preference for highly-symmetric states could hold the key for understanding this phenomenon. Since the intrinsic momentum scales in these channels are so small, one may recover them by expanding about scale zero, namely about Unitarity.

Let us first address the importance of Unitarity in general terms. The centre-of-mass two-body scattering amplitude at relative momentum k is

$$A(k) = \frac{4\pi}{M} \frac{1}{k \cot \delta(k) - ik} . \quad (1.1)$$

The term “ $-ik$ ” ensures Unitarity of the S matrix, *i.e.* probability conservation. The function $k \cot \delta(k)$ parametrises the part which encodes all information on the interactions.

For $|k \cot \delta| \gtrsim |ik|$, the phase shift is “small”, $|\delta(k)| \lesssim 45^\circ$, so that contributions from interactions are small and can be treated perturbatively (Born approximation):

$$A(k) \Big|_{\text{Born}} = \frac{4\pi}{M} \frac{1}{k \cot \delta(k)} \left[1 + \frac{i}{\cot \delta(k)} + \mathcal{O}(\cot^{-2} \delta) \right] . \quad (1.2)$$

In this **Born Corridor**, details of the interactions enter at LO and are therefore crucial.

On the other hand, in the **Unitarity Window** $|k \cot \delta| \lesssim |ik|$ about the Unitarity Point $\cot \delta = 0$, the phase shift is “large”, $45^\circ \lesssim |\delta(k)| \lesssim 135^\circ$. Albeit interactions are so strong that they must be treated non-perturbatively at leading order by resumming an infinite iteration, Unitarity actually dominates the amplitude:

$$A(k) \Big|_{\text{Uni}} = \frac{4\pi}{M} \frac{1}{-ik} \left[1 + \frac{\cot \delta(k)}{i} + \frac{\cot^2 \delta(k)}{i^2} + \mathcal{O}(\cot^3 \delta) \right] . \quad (1.3)$$

This seems paradoxical, but the interactions are actually so strong that their details do not matter as much as the simple fact that they are very strong – so strong indeed that

probability conservation limits their impact on observables. For example, the cross section is saturated, $\sigma = \frac{4\pi}{k^2}[1 + \mathcal{O}(\cot\delta)]$. Moreover, an anomalously shallow bound state emerges naturally since the amplitude's pole is at zero, $k_{\text{pole}} = 0 + \mathcal{O}(\cot\delta)$. Since the leading amplitude has no intrinsic scale, all dimensionless observables are zero or infinite at LO, while all dimensionful quantities (like the cross section) are homogeneous functions of k . Their exponents are set by dimensional analysis, and their dimensionless coefficients are universal (*i.e.* interaction-independent). Therefore, Unitarity and Universality are closely related: Differences between systems at Unitarity can only come from different symmetry properties of the Unitarity Point itself but are universal otherwise; this will be important for imposing a dominant symmetry in the final part of the Conclusions.

Universality, in turn, has been proposed as key to the emergence of simple, unifying patterns in complex systems like the nuclear chart [6–11]. These articles showed that the expansion about Unitarity reproduces indeed fundamental patterns on a quantitative level, like the binding of the ${}^4\text{He}$ nucleus and its shallow first excitation. This led to indications that it describes heavier systems and nuclear matter [12–17]; see also [18, 19] for reviews.

The transition between Born Corridor and Unitarity Window is of course gradual rather than abrupt. One would expect computations of observables to still be reliable to some degree as one intrudes into the other. The borders should therefore not be taken literally but are fuzzily located around phase shifts of about 45° and 135° ($|\cot\delta| \approx 1$).

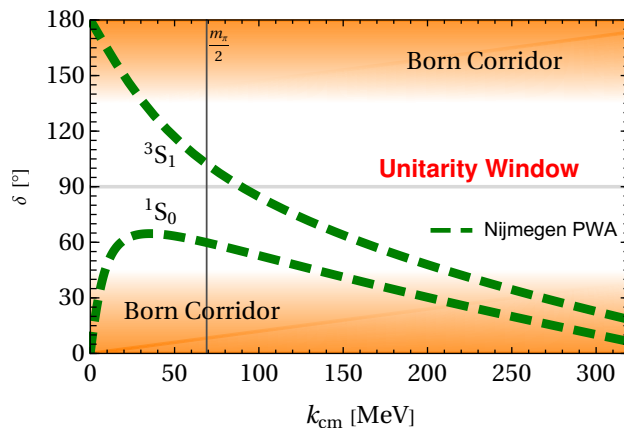


Figure 1: (Colour on-line) Born Corridor and Unitarity Window of NN phase shifts in the ${}^1\text{S}_0$ and ${}^3\text{S}_1$ channels in the Nijmegen PWA [20]. Marked is also the scale associated with the first non-analyticity in $k\cot\delta(k)$, from the branch point $k = \pm i\frac{m_\pi}{2}$ of OPE.

So is the Unitarity Window relevant in NN? According to Partial-Wave Analyses (PWAs) [20–23]¹, only two channels are clearly inside at momenta relevant for low-energy properties of systems of nucleons, namely $k \lesssim 300$ MeV (lab energies $\lesssim 200$ MeV): ${}^1\text{S}_0$ and ${}^3\text{S}_1$. According to fig. 1, they are clearly inside the Unitarity Window for $40 \text{ MeV} \lesssim k \lesssim$

¹While we use the Nijmegen PWA, uncertainties are minuscule in these channels. The ${}^1\text{S}_0$ and ${}^3\text{SD}_1$ phase shifts and mixing angles reported by the Granada group differ by less than 0.6° up to $k = 350$ MeV.

200 MeV. This estimate is conservative, and the boundaries are again to be understood as fuzzy. This and their shallow bound states motivate starting from Unitarity.

While 3S_1 is part of a coupled channel, the magnitudes of the 3SD_1 mixing angle and 3D_1 phase shifts do not exceed 25° and may be amenable to treatment in perturbation. The $^3P_{0,2}$, 3P_1 and 3D_2 channels hardly reach 25° , either. The degree to which they must be treated nonperturbatively at LO is under dispute. The other partial waves have even smaller phase shifts and can easily be described in perturbation [24–27].

Unitarity is so attractive because its two-nucleon state is highly symmetric. Both 1S_0 and 3S_1 amplitudes are scale-invariant and thus identical, *i.e.* invariant under Wigner’s combined-SU(4) spin and isospin rotations [28–30], up to differences in scattering-length and effective-range corrections; see [31, 32] for numerical evidence in phenomenological NN potentials. The tightest-bound light nuclei, ^4He , ^{12}C and ^{16}O , are all near-perfect spin-isospin-singlets. In QCD’s large- N_C expansion, the leading non-tensor part of the NN interaction is automatically Wigner-SU(4) symmetric in even partial waves [33, 34]; *cf.* [35, 36] for a concise summary. [We return to the interplay with large- N_C in the Conclusions.]

While one can only surmise that Nature prefers expansions about configurations with very high degrees of symmetry, theorists certainly do: Noether’s theorem [37] relating continuous symmetries to conserved quantities and currents is a cornerstone of modern Physics. Since $\infty \neq |a(^1S_0)| \neq |a(^3S_1)| \neq \infty$, both scale invariance and Wigner-SU(4) symmetry are weakly broken in Nature at momenta for which $|\text{kcot}\delta| < 1$ and the **Unitarity Expansion** should be useful as expansion about a nontrivial renormalisation-group fixed point with a high degree of symmetry [26, 27, 38, 39]. This fixed point is fully characterised by the fact that it is nontrivial, and by its symmetries: scaling and Wigner-SU(4) invariance in systems of 2 and more nucleons. Its natural renormalisation point is the momentum $k = 0$ itself. We will use it for our main results but also vary it to see the impact on our conclusions.

In the language of Information Theory, the high degree of symmetry at Unitarity means that the existence of anomalous scattering lengths is important, while their values are demoted to be of less consequence, on par with other information (like from effective ranges). This optimises “lossless compression” of relevant information and suppresses irrelevant one.

Wigner-SU(4) symmetry plays a prominent rôle in “Pionless EFT” (EFT($\not{\pi}$)). Its 3N Counter Term (CT) needed to renormalise LO is automatically spin-isospin invariant, with its Low-Energy-Coefficient (LEC) fixed by a 3N datum [40]. Other examples include classifying parity-violating and conserving 3N interactions [41–44]; and patterns in nuclear systems [45–47], like the ^{12}C ground and Hoyle states [48].

The first non-analyticity in $\text{kcot}\delta$ comes from the longest-range nonlocal exchange interaction, namely OPE. The scale $k \sim \frac{m_\pi}{2}$ associated with its left-hand branch point at $k = \pm i\frac{m_\pi}{2}$ lies not just well inside the Unitarity Window, as fig. 1 shows. It also appears to be right around where both partial waves are close to perfect Unitarity, $\delta = 90^\circ$.

This non-analyticity signals the formal breakdown scale of EFT without explicit pionic degrees of freedom, *i.e.* its mathematica radius of convergence. And yet, it is of all EFTs the only one for which the Unitarity Expansion has thus far been explored [7–10, 12, 17, 18]. That its formal convergence radius does not cover the full Unitarity Window is only mitigated by the well-documented fact that it appears to converge much better in practical

applications. For example, a recent Bayesian order-by-order convergence analysis put its breakdown scale with 68% degree of belief (DoB) at $[0.96; 1.69] m_\pi$ [49]. The tension between the extent of the Unitarity Window, and the breakdown of analyticity and practical convergence of EFT(\not{x}), makes one ask how the Unitarity Expansion emerges in χ EFT, *i.e.* with pionic degrees of freedom automatically embedding the non-analyticities [50]. How big is the window in which χ EFT about Unitarity is both valid and efficiently describes data?

Pions add however another issue. The long-range OPE interaction dominates between nucleons [\vec{e}_q : unit vector of momentum transfer \vec{q} ; $\vec{\sigma}_i, \vec{\tau}_i$: nucleon i 's spin, isospin]:

$$V_{\text{OPE}} = -\frac{g_A^2}{12f_\pi^2} \frac{\vec{q}^2}{\vec{q}^2 + m_\pi^2} \left[(\vec{\sigma}_1 \cdot \vec{\sigma}_2) + [3(\vec{\sigma}_1 \cdot \vec{e}_q)(\vec{\sigma}_2 \cdot \vec{e}_q) - (\vec{\sigma}_1 \cdot \vec{\sigma}_2)] \right] (\vec{\tau}_1 \cdot \vec{\tau}_2) \quad (1.4)$$

$$=: (\vec{\sigma}_1 \cdot \vec{\sigma}_2) (\vec{\tau}_1 \cdot \vec{\tau}_2) V_C + [3(\vec{\sigma}_1 \cdot \vec{e}_q)(\vec{\sigma}_2 \cdot \vec{e}_q) - (\vec{\sigma}_1 \cdot \vec{\sigma}_2)] (\vec{\tau}_1 \cdot \vec{\tau}_2) V_T .$$

The pion decay constant f_π and m_π break scale invariance explicitly because they carry mass dimensions. On top of that, the spin-isospin structure of the tensor part, V_T , manifestly breaks Wigner-SU(4) symmetry. On the other hand, that of the central part, V_C , is manifestly Wigner-symmetric, *i.e.* its contribution to OPE is identical the 1S_0 and 3S_1 channels. It is also the *only* contribution in the 1S_0 channel since the tensor piece is of course identical zero there. Therefore, only amplitudes without V_T are Wigner-invariant, while those with at least one V_T automatically break the symmetry. Consequently, it is not self-understood how explicit pionic degrees of freedom can be reconciled with the symmetries of the Unitarity Expansion which they appear to break rather strongly, while concurrently extending the applicable range to the whole Unitarity Window, including $k \gtrsim m_\pi$.

We choose to investigate the transition between “pionless” and “pionic” EFT by employing χ EFT “with Perturbative/KSW Pions”, proposed by Kaplan, Savage and Wise [51, 52]. In it, LO consists still only of iterated contact interactions without momentum dependence. Together with corrections to these, OPE without iteration enters at NLO, and once-iterated OPE at N²LO. Twice-iterated OPE as well as correlated two-pion exchange is relegated to higher orders. Its natural breakdown scale $\bar{\Lambda}_{\text{NN}}$ is thus set by the scale of OPE [51–53], and its dimensionless expansion parameter Q with typical momentum scale $p_{\text{typ}} \sim k, m_\pi$ is

$$Q = \frac{p_{\text{typ}}}{\bar{\Lambda}_{\text{NN}}} \quad \text{with} \quad \bar{\Lambda}_{\text{NN}} = \frac{16\pi f_\pi^2}{g_A^2 M} \approx 300 \text{ MeV} . \quad (1.5)$$

While numerically $\bar{\Lambda}_{\text{NN}} \approx 2m_\pi$ at physical pion masses, it does not explicitly depend on m_π and is therefore largely constant in the chiral limit. However, Fleming, Mehen and Stewart (FMS) found [53, 54] that perturbative pions at N²LO fit 3S_1 phase shifts rather poorly for $k \gtrsim 140$ MeV, *i.e.* well below $\bar{\Lambda}_{\text{NN}}$, and order-by-order convergence was elusive. And yet, this is the only χ EFT which is known to be self-consistent and renormalisable order by order, with a well-understood power counting [25]. Therefore, it is still employed when predictions in the absence of data must be made, *e.g.* in beyond-the-standard-model processes [55–57]. Modification with better convergence properties have also been explored [58, 59].

We count powers of Q throughout as follows. In an EFT with resummed LO in the 2-body system, LO must for consistency on general grounds be counted as $\mathcal{O}(Q^{-1})$; see *e.g.* [60, 61].

We identify next-to-leading order (NLO) with $\mathcal{O}(Q^0)$, and next-to-next-to-leading order N²LO with $\mathcal{O}(Q^1)$. With perturbative pions, none of these is zero. We are interested in the Unitarity Window of the two-nucleon system, *i.e.* $\frac{1}{|a|} \ll k \ll \bar{\Lambda}_{\text{NN}}$. For the sake of simplicity, we equate two dimensionless expansion parameters, $Q := \frac{k, m_\pi \sim r^{-1}}{\bar{\Lambda}_{\text{NN}}} \approx \frac{1}{ka} \rightarrow Q$, since they are numerically close for $k \approx m_\pi$ and physical values of the NN scattering length.

We thus propose the **$\chi\text{EFT with Perturbative Pions in the Unitarity Expansion}$** (**$\chi\text{EFT}(\text{p}\pi)_{\text{UE}}$**). Its N²LO amplitudes are based on the work by Rupak and Shores in the $^1\text{S}_0$ channel [62] and by FMS in $^3\text{SD}_1$ [53, 54]. We will argue that it has a much wider range of both convergence and agreement with PWAs than EFT(π), if the following holds:

Hypothesis: The symmetries of the Unitarity limit are broken weakly in Nuclear Physics. Their footprint shows *persistence*, *i.e.* their impact dominates observables at momentum scales $p_{\text{typ}} \sim m_\pi$ and beyond, and is more relevant than chiral symmetry. In particular, the tensor/Wigner-SU(4) symmetry-breaking part of one-pion exchange in the NN $^3\text{S}_1$ channel is super-perturbative, *i.e.* does not enter before N³LO.

Co-author Teng’s MSc thesis gave first results in 2023 [63]. Recently, we discussed findings and Hypothesis at the ECT* workshop *The Nuclear Interaction: Post-Modern Developments*, the *11th International Workshop on Chiral Dynamics (CD2024)*, and INT programme *INT-24-3 Quantum Few- and Many-Body Systems in Universal Regimes* [64–66].

This article is organised as follows. Section 2 is devoted to methodology. EFT(π) in the Unitarity Expansion (sect. 2.1) illustrates issues in extracting the phase shifts, $k\cot\delta$ (sect. 2.2), pole positions and residues (sect. 2.3). Section 2.4 discusses the χEFT amplitudes with Perturbative Pions in the Unitarity Expansion at $\mathcal{O}(Q^1)$ (N²LO). It identifies the Wigner-SU(4) invariant parts (sect. 2.4.1) and specifies renormalisation point and parameters (sect. 2.4.2). Section 3 on the results starts with the zero-momentum and pole properties. Our central results are sects. 3.2 on the $^1\text{S}_0$ channel and 3.3 on the full $^3\text{S}_1$ channel both with and without its Wigner-SU(4) breaking part. A detailed accounting of theory uncertainties is given in sect. 3.5: order-by-order convergence, expansion parameters inside the Unitarity Window, convergence to the PWA, and complementing phase shift extractions, all summarised and compared in sect. 3.5.6. We discuss varying the fit point in sect 3.6. The customary summary and outlook in sect. 4 adds a discussion of the interplay of Wigner symmetry with QCD’s large- N_C limit and restates the Hypothesis: The Unitarity limit’s symmetries persist and dominate well into a momentum régime in which pions should be accounted for.

2 Amplitudes and Observables

2.1 Amplitudes in Pionless EFT

To set up $\chi\text{EFT}(\text{p}\pi)_{\text{UE}}$, we consider the Unitarity Expansion at very low energies. That is the régime of EFT(π), which is at N²LO identical to the Effective Range Expansion (ERE) [67–70]. We will use it in sect. 3 to check how important pions actually are. In addition, some

subtleties on extracting observables in the next subsection becomes more transparent. The function $\text{kcot}\delta(k)$ which parametrises the interaction part has an expansion in powers of k^2 for $k \lesssim \frac{m_\pi}{2}$, *i.e.* below non-analyticities from non-iterated OPE:

$$\text{kcot}\delta(k) = -\frac{1}{a} + \frac{r}{2} k^2 + \sum_{n=2}^{\infty} v_n k^{2n} , \quad (2.1)$$

with a the scattering length, r the effective range, v_n the shape parameters². From fig. 1, phase shifts are inside the Unitarity Window even at these low momenta, so we choose:

$$\text{kcot}\delta_{0,-1}^\pi = 0 , \quad \text{kcot}\delta_{0,0}^\pi = \left(\frac{1}{a} - \frac{r}{2} k^2 \right) , \quad \text{kcot}\delta_{0,1}^\pi = 0 . \quad (2.2)$$

The first subscript denotes the S channel ($l=0$); the second the order in Q . Inserting into the Unitarity Expansion, eq. (1.3), one finds at $\mathcal{O}(Q^1)$ (N²LO):

$$A_{-1\pi}^{(S)}(k) = \frac{4\pi i}{M} \frac{1}{k} , \quad A_{0\pi}^{(S)}(k) = -\frac{4\pi}{Mk} \left(\frac{1}{ka} - \frac{kr}{2} \right) , \quad A_{1\pi}^{(S)}(k) = \frac{[A_{0\pi}^{(S)}(k)]^2}{A_{-1\pi}^{(S)}(k)} . \quad (2.3)$$

We therefore summarise that the Unitarity Expansion proceeds in powers of Q and holds as long as $Q \sim \frac{1}{ka}, \frac{rk}{2} \ll 1$. This also implies $Q^2 \sim \frac{r}{2a} \ll 1$, *i.e.* r is of natural size if a is anomalously large. It breaks down for momenta which are either small, $k \lesssim \frac{1}{a}$, or large, $k \gtrsim \frac{2}{r}$, relative to the ERE scales. The dimensionless expansion parameters at, for example, $k \approx \frac{m_\pi}{2}$ are $\frac{1}{ka(^1S_0)} \approx 0.1$, $\frac{1}{2}kr(^1S_0) \approx 0.5$, $\frac{1}{ka(^3S_1)} \approx 0.5$ and $\frac{1}{2}kr(^3S_1) \approx 0.3$. Since none of these are particularly small, convergence in observables must carefully be assessed; see sect. 3.5. The two NLO contributions are of size $|\frac{ar}{2} k^2|$ relative to each other. For $k \approx \frac{m_\pi}{2}$, this is ≈ 4 in 1S_0 and ≈ 0.6 . So we follow [7] to define expansions about Unitarity such that $\mathcal{O}(Q^0)$ (NLO) includes both the scattering length and effective range. At higher k , r dominates against a , so that the latter could be considered N²LO, but we strive for an expansion which applies throughout the Unitarity Window.

Notice that no new Physics enters at N²LO since the amplitude is entirely determined by the LO and NLO results. The coefficients $v_n \sim m_\pi^{-2n+1}$ are assumed to be of natural size. The first additional datum comes then from the shape parameter v_2 at $\mathcal{O}(Q^2)$ (N³LO), *i.e.* one order higher than considered here. Additional information from v_n enters at $\mathcal{O}(Q^{2n-2})$ (N²ⁿ⁻¹LO). No new information enters at odd powers of Q (even N^mLO).

2.2 From Amplitudes to Phase Shifts

In a perturbative calculation, converting an amplitude into observables is dictated by the theorems of Mathematical Perturbation Theory [71–74]. Only an order-by-order expansion in both amplitude and observable is guaranteed to preserve the symmetries (including Unitarity of the S matrix) at each order independently. Different paths to observables all must

²Other conventions include $v_n = -P_n r^{2n-1}$ with dimensionless P_n and factors of 2, 4 and $n!$.

at a given order agree to within uncertainties associated with the next order not retained. Therefore, we will in sect 3.5 use different extractions of the same observable to estimate the truncation uncertainties and order-by-order convergence.

First, we follow the original KSW/FMS prescription from the S matrix. Its Stapp-Ypsilanti-Metropolis (SYM/"bar") parametrisation [75] is also used by the Nijmegen [20] and Granada [21–23] PWAs. The scattering matrix in the coupled $^3\text{SD}_1$ channel is

$$S = \mathbb{1} + \frac{ikM}{2\pi} \begin{pmatrix} A^{(\text{SS})} & A^{(\text{SD})} \\ A^{(\text{SD})} & A^{(\text{DD})} \end{pmatrix} = \begin{pmatrix} e^{2i\delta_0} \cos 2\varepsilon & ie^{i(\delta_0+\delta_2)} \sin 2\varepsilon \\ ie^{i(\delta_0+\delta_2)} \sin 2\varepsilon & e^{2i\delta_2} \cos 2\varepsilon \end{pmatrix} . \quad (2.4)$$

Throughout, the $^1\text{S}_0$ case is retrieved by setting $\delta_2 = \varepsilon = 0$, $A^{(\text{SD})} = A^{(\text{DD})} = 0$.

Like the amplitudes $A = A_{-1} + A_0 + A_1 + A_2 \dots$, each phase shift and the mixing angle ε is expanded in powers of the small, dimensionless parameter:

$$\delta_0 = \delta_{0,-1} + \delta_{0,0} + \delta_{0,1} + \delta_{0,2} + \dots \text{ and likewise for } \delta_2, \varepsilon_1 , \quad (2.5)$$

where $\delta_{0,-1} \gg \delta_{0,0} \gg \delta_{0,1} \gg \delta_{0,2} \dots$ and the second subscript denotes again the order in Q . In χEFT with Perturbative Pions, only the S wave phase shift is nonzero at LO, while $\delta_{2,-1} = \varepsilon_{2,-1} = 0$ vanish. Expanding and matching order-by-order, we quote the result from KSW/FMS [52, 53]. The only nonzero LO contribution is

$$\delta_{0,-1} = -\frac{i}{2} \ln \left[1 + \frac{ikM}{2\pi} A_{-1}^{(\text{SS})} \right] . \quad (2.6)$$

At NLO and N^2LO , one adds for the S wave phase shifts

$$\delta_{0,0} = \frac{kM}{4\pi} \frac{A_0^{(\text{SS})}}{1 + \frac{ikM}{2\pi} A_{-1}^{(\text{SS})}} , \quad (2.7)$$

$$\delta_{0,1} = \frac{kM}{4\pi} \frac{A_1^{(\text{SS})} - i \frac{kM}{4\pi} [A_0^{(\text{SD})}]^2}{1 + \frac{ikM}{2\pi} A_{-1}^{(\text{SS})}} - i (\delta_{0,0})^2 . \quad (2.8)$$

While the SD-mixing NLO amplitude $A_0^{(\text{SD})}$ enters at N^2LO , sect. 2.4.5 shows that it cancels in the $^3\text{S}_1$ channel against terms in $A_1^{(\text{SS})}$. Formulae for δ_2 and ε can be found in [52–54, 63].

In the Unitarity limit, the term in the denominators simplifies to $1 + \frac{ikM}{2\pi} A_{-1}^{(\text{SS})}|_{\text{Uni}} = -1$ and the LO phase shift is in both S waves as expected identically

$$\delta_{0,-1} \equiv \frac{\pi}{2} = 90^\circ . \quad (2.9)$$

However, from the pionless amplitudes of eq. (2.3), the NLO correction,

$$\delta_{0,0} = \frac{1}{ka} - \frac{kr}{2} , \quad (2.10)$$

suffers an apparent divergence for $1 \gg ka \rightarrow 0$. The same holds for $\chi\text{EFT}(\text{p}\pi)_{\text{UE}}$. Strictly speaking, this is not an issue since such a limit is outside the window $\frac{1}{ka} \lesssim 1$ in which the

Unitarity Expansion converges. Still, the divergence may obscure features close to $k = 0$ which can be of interest. Ultimately, its origin is a mismatch between defining the low-energy parameters in the ERE of $\text{kcot}\delta$, eq. (2.1), and the constraint that $\delta(k \rightarrow 0) \rightarrow 0$ or 180° at NLO and in physical systems, while the value is 90° at Unitarity.

We therefore use another definition which expands not the phase shifts but the “physical” part of the amplitude, *i.e.* $\text{kcot}\delta$ as in eq. (1.3): Replace phase shifts ($l = 0, 2$) by

$$e^{2i\delta_l} = 1 + \frac{2ik}{\text{kcot}\delta(k) - ik} \text{ with } \text{kcot}\delta = \text{kcot}\delta_{l,-1} + \text{kcot}\delta_{l,0} + \text{kcot}\delta_{l,1} + \text{kcot}\delta_{l,2} + \dots, \quad (2.11)$$

expand the mixing parameter ε as before, use that $\text{kcot}\delta_{2,-1} = 0$ vanishes at LO, and find at LO, NLO and N²LO, respectively (see also ref. [62] for $^1\text{S}_0$):

$$\text{kcot}\delta_{0,-1} = ik + \frac{4\pi}{M} \frac{1}{A_{-1}^{(\text{SS})}} \quad (2.12)$$

$$\text{kcot}\delta_{0,0} = -\frac{4\pi}{M} \frac{A_0^{(\text{SS})}}{[A_{-1}^{(\text{SS})}]^2} \quad (2.13)$$

$$\text{kcot}\delta_{0,1} = -\frac{4\pi}{M} \left(\frac{A_1^{(\text{SS})}}{[A_{-1}^{(\text{SS})}]^2} - \frac{[A_0^{(\text{SS})}]^2}{[A_{-1}^{(\text{SS})}]^3} \right) + ik \frac{[A_0^{(\text{SD})}]^2}{[A_{-1}^{(\text{SS})}]^2} \quad (2.14)$$

Deriving the corresponding formulae for $\text{kcot}\delta_2$ and ε is again straightforward [63].

The phase shifts are then simply found by inverting $\text{kcot}\delta_0$ at the appropriate order. In the Unitarity limit, the LO expression is as expected

$$\text{kcot}\delta_{0,-1}|_{\text{Uni}} = 0, \quad (2.15)$$

i.e. $\delta_{0,-1}(k) = \text{arccot}[\frac{0}{k}] \equiv \frac{\pi}{2} = 90^\circ$. Now, one finds at NLO in pionless EFT from eq. (2.3) by construction the effective-range result:

$$\text{kcot}\delta_{0,0}|_{\text{Uni}} = -\frac{1}{a} + \frac{r}{2}k^2 \implies \delta_0 = \text{arccot}\left[\frac{0 - \frac{1}{a} + \frac{r}{2}k^2}{k}\right] \xrightarrow{k \rightarrow 0} \arctan 0. \quad (2.16)$$

This is finite (0° for $a < 0$, 180° for $a > 0$) and reproduces at NLO the first two terms of ERE and EFT($\not\pi$) (2.1). The $\mathcal{O}(Q^n)$ (N ^{$n+1$} LO) terms are (also beyond Unitarity Expansion)

$$\text{kcot}\delta_{0,n} = \begin{cases} \frac{v_{n+2}}{2} k^{n+2} & \text{for } n \geq 2 \text{ even} \\ 0 & \text{for } n \geq 1 \text{ odd} \end{cases}. \quad (2.17)$$

Since the N²LO contribution vanishes, we refer to such results as “EFT($\not\pi$) NLO=N²LO”.

In the following, we will mostly use the $\text{kcot}\delta$ form, cognisant of the fact that phase shifts at $\frac{1}{ka} \gtrsim 1$ are outside the Unitarity Window. In both variants to extract phase shifts, as in all expansions which are consistent within Mathematical Perturbation Theory, all phase shifts $\delta_0, \delta_2, \varepsilon$ as well as $\text{kcot}\delta$ are at each order real below the pion-production threshold, *i.e.* S -matrix unitarity is manifest at each order. In sect. 3.5, we will compare both versions to assess truncation uncertainties and radius of convergence.

2.3 From Amplitudes to Pole Positions

Poles of the S matrix, and hence of the amplitudes, at complex momentum $i\gamma$ correspond to real bound states for $\text{Re}[\gamma] > 0, \text{Im}[\gamma] = 0$; to virtual states for $\text{Re}[\gamma] < 0, \text{Im}[\gamma] = 0$, and to resonances for $\text{Re}[\gamma] < 0, \text{Im}[\gamma] \neq 0$. Unitarity is at $\gamma = 0$. Nonrelativistically, the corresponding (real or virtual) binding energies are $B = \frac{\gamma^2}{M} > 0$ when bound.

Extracting bound state properties from amplitudes is again well-defined in Mathematical Perturbation Theory [71–74]; see also [62, 76] and a technical summary [77]. Poles are zeroes of the inverse S matrix (or amplitude) and must appear in all coupled waves concurrently. It suffices to consider the zeroes of the denominator in eq. (2.11). In addition to the function $\text{kcot}\delta(k)$, one also expands the pole position, *i.e.* its argument:

$$k_{\text{pole}} = i(\gamma_{-1} + \gamma_0 + \gamma_1 + \dots) . \quad (2.18)$$

Likewise, the (rescaled) residue at the pole is found by expanding

$$Z^{-1} = \frac{4\pi i}{M} \frac{d}{dk} \frac{1}{A(k)} \Big|_{k=i\gamma} = i \frac{d}{dk} (\text{kcot}\delta_0(k) - ik) \Big|_{k=i\gamma} . \quad (2.19)$$

For ease of notation, we also define the m th derivative of the n th ($\mathcal{O}(Q^n)$, $N^{n+1}\text{LO}$) contribution to $\text{kcot}\delta_0$ at $k = i\gamma_{-1}$ as $\text{kcot}\delta_{0,n}^{(m)}(i\gamma_{-1}) := \frac{d^m \text{kcot}\delta_{0,n}(k)}{dk^m} \Big|_{k=i\gamma_{-1}}$. The leading-order pole position is determined implicitly, and the residue is fixed by the Unitarity part, ik :

$$\text{kcot}\delta_{0,-1}(i\gamma_{-1}) + \gamma_{-1} \stackrel{!}{=} 0 \quad , \quad (Z_{-1})^{-1} = 1 + i \text{kcot}\delta_{0,-1}^{(1)}(i\gamma_{-1}) . \quad (2.20)$$

The other orders are again solved by iteration:

$$i\gamma_0 = \frac{\text{kcot}\delta_{0,0}(i\gamma_{-1})}{i - \text{kcot}\delta_{0,-1}^{(1)}(i\gamma_{-1})} \quad (2.21)$$

$$i\gamma_1 = \frac{i\gamma_0}{\text{kcot}\delta_{0,0}(i\gamma_{-1})} \left(\text{kcot}\delta_{0,1}(i\gamma_{-1}) + i\gamma_0 \text{kcot}\delta_{0,0}^{(1)}(i\gamma_{-1}) + \frac{(i\gamma_0)^2}{2} \text{kcot}\delta_{0,-1}^{(2)}(i\gamma_{-1}) \right) \quad (2.22)$$

For expressions via amplitudes, one starts from $[A_{-1}(k_{\text{pole}}) + A_0(k_{\text{pole}}) + \dots]^{-1} \stackrel{!}{=} 0$ or inserts eqs. (2.12) to (2.14). Usually, $\text{kcot}\delta$ is analytic in k^2 around γ_{-1} , so that $\text{kcot}\delta_{0,n}^{(m)}(i\gamma_{-1}) = 0$ for odd $n \geq 1$ from eq. (2.17). In the Unitarity Expansion ($\gamma_{-1} = 0$), $\text{kcot}\delta_{0,-1} \equiv 0 \equiv \text{kcot}\delta_{-1\text{p}}^{(m)}$ vanishes with all its derivatives, and the last term in parenthesis is zero.

Expanding the residue is straightforward; we only quote the next nontrivial term:

$$Z_0 = -i(Z_{-1})^2 \left(\text{kcot}\delta_{0,0}^{(1)}(i\gamma_{-1}) + i\gamma_0 \text{kcot}\delta_{0,-1}^{(2)}(i\gamma_{-1}) \right) . \quad (2.23)$$

That both the Unitarity limit and ERE/EFT(π) expand about the same point $k = 0$ has a curious consequence. Since $\text{kcot}\delta$ is there analytic in k^2 , one can use directly eq. (2.1). All odd orders of γ_n and all even orders of Z_n are zero. The first nonzero terms are:

$$i\gamma_0 = \frac{i}{a} \quad , \quad i\gamma_2 = \frac{ir}{2a^2} \quad , \quad i\gamma_4 = \frac{ir^2}{2a^3} \quad , \quad i\gamma_6 = \frac{i}{2a^4} \left(\frac{5r^3}{4} - 2v_2 \right) \quad (2.24)$$

$$Z_{-1} = 1 \quad , \quad Z_1 = \frac{r}{a} \quad , \quad Z_3 = \frac{3r^2}{2a^2} \quad , \quad Z_5 = \frac{1}{2a^3} (5r^3 - 8v_2) \quad (2.25)$$

[The first term in each line and $i\gamma_1 = 0 = Z_0$ also follow from inserting the pionless amplitudes of eq. (2.3) into eqs. (2.21) and (2.22).] These series converge since $\frac{r}{a} \ll 1$ inside the Unitarity Window and we assume $v_n \sim m_\pi^{-2n+1}$ are natural as well.

While the shape parameter v_2 enters at $\mathcal{O}(Q^2)$ (N³LO) in ERE/EFT(\not{x}), it shifts the pole only at a very high $\mathcal{O}(Q^6)$ (N⁷LO) when the parameters of the Unitarity Expansion are determined at $k = 0$. The reason is that $\text{kcot}\delta_{0,n}(k) \propto k^{2n+2}$ beyond NLO, so that at zero momentum $\text{kcot}\delta_{0,n}^{(m)}(0) = 0$ – unless $m = 2n + 2$ so that $\text{kcot}\delta_{0,n}^{(2n+2)}(0) = (2n + 2)! \frac{v_{n+2}}{2}$. This is inconsequential as long as all derivatives and functions in the pole expansion must be taken at a LO pole position $\gamma_{-1} \neq 0$. But Unitarity mandates $i\gamma_{-1} = 0$, so nearly all contributions to the pole momentum disappear. As a consequence, the binding momentum and residue can be determined to quite high order in the Unitarity Expansion, even if the ERE is given only to N²LO (expanding in $\sqrt{\frac{r}{a}}$ would induce non-analyticities in r, a):

$$i\gamma = \frac{i}{a} \left(1 + \frac{r}{2a} + \frac{r^2}{2a^2} + \mathcal{O}\left(\frac{r^3}{a^3}\right) \right) \quad (2.26)$$

$$Z = 1 + \frac{r}{a} + \frac{3r^2}{2a^2} + \mathcal{O}\left(\frac{r^3}{a^3}\right) \quad (2.27)$$

This result is accurate only up to and including N²LO in $\frac{r}{a}$. It coincides with the outcome of ERE/EFT(\not{x}) without Unitarity Expansion at N²LO. When the scattering length is included at LO (instead of NLO as in the Unitarity Expansion), terms with n powers of $\frac{1}{a} \sim Q^{-1}$ are merely reshuffled to n orders earlier, leading to $i\gamma_{-1}^{\text{trad}} = i\gamma_0$, $i\gamma_0^{\text{trad}} = i\gamma_2$, $Z_0^{\text{trad}} = Z_1$ etc.

Under the assumptions in sect. 3.5.4, the “max” criterion estimates truncation uncertainties quantitatively [78, sect. 4.4]. A Bayesian analysis with reasonable priors on the coefficients of the expansion [79–81] asserts a 68% degree-of-belief (DoB) interval of $\pm \frac{i}{a} \frac{r^3}{2a^3}$ for the pole position and $\pm \frac{3r^3}{2a^3}$ for its residue. For EFT(\not{x}) in the ¹S₀ and ³S₁ channels, the pole positions and residues are then (errors from empirical values are negligible):

$$\begin{aligned} i\gamma(^1\text{S}_0) &= [-7.898 \pm 0.006]i \text{ MeV} & , & \quad Z(^1\text{S}_0) = [0.906 \pm 0.002] \\ \text{empirical:} & [-7.892 \pm 0.040]i \text{ MeV} & , & \quad [0.9034 \pm 0.0005] \\ i\gamma(^3\text{S}_1) &= [+44.6 \pm 0.7]i \text{ MeV} & , & \quad Z(^3\text{S}_1) = [1.515 \pm 0.06] \\ \text{empirical:} & [+45.7023 \pm 0.0001]i \text{ MeV} & , & \quad [1.6889 \pm 0.0031] \end{aligned} \quad (2.28)$$

This compares within uncertainties favourably to the empirical values. In the ³S₁ channel, these were derived from the binding energy and asymptotic normalisation of the deuteron ($\gamma = \sqrt{MB_2}$, $Z = \frac{A_2^2}{2\gamma}$) reported by the Granada group [23]. For the ¹S₀ channel, these are inferred from the Granada group’s values of the scattering length, effective range and shape parameter of sect. 2.4.2, as described in [82].

We presented some details of this analysis since sect. 3.1 will demonstrate that the same postdiction emerges in $\chi\text{EFT}(\text{p}\pi)_{\text{UE}}$ at renormalisation point $k = 0$.

2.4 Amplitudes in χ EFT with Perturbative Pions about Unitarity

2.4.1 Wigner-SU(4) Symmetry in χ EFT($p\pi$)_{UE}

To facilitate later discussions, we first identify those Wigner-SU(4) symmetric and breaking parts of χ EFT($p\pi$)_{UE} in the 1S_0 and 3S_1 channels. LO eigenstates $|^3S_1\rangle$, $|^1S_0\rangle$ are pure 3S_1 and 1S_0 waves. As discussed in the Introduction, the central part of OPE, V_C , is Wigner-SU(4) invariant, while the tensor piece, V_T , breaks it. At NLO, OPE is inserted once. Symbolically, we can therefore use the well-known projection of V_{OPE} (with corresponding contact terms for renormalisation) onto the 1S_0 and 3S_1 channels:

$$\begin{aligned} A_0(^1S_0) &= \langle ^1S_0 | V_C | ^1S_0 \rangle =: A_0^S \\ A_0(^3S_1) &= \begin{pmatrix} |^3S_1\rangle \\ 0 \end{pmatrix}^\dagger \begin{pmatrix} V_C & \sqrt{8} V_T \\ \sqrt{8} V_T & V_C - 2V_T \end{pmatrix} \begin{pmatrix} |^3S_1\rangle \\ 0 \end{pmatrix} = \langle ^3S_1 | V_C | ^3S_1 \rangle = A_0^S \end{aligned} \quad (2.29)$$

where we used that the LO eigenstates are Wigner-SU(4) invariant, $|^3S_1\rangle = |^1S_0\rangle$. We introduce A_0^S for the NLO amplitude and $A_{1\text{sym}}^S$ ($A_{1\text{break}}^S$) for invariant (breaking) amplitudes, with the subscript indicating a $\mathcal{O}(Q^n)$ ($N^{n+1}\text{LO}$) contribution.

The pion contribution at NLO is therefore Wigner-SU(4) symmetric. Pion-exchange induced differences between the partial waves only enter at $N^2\text{LO}$:

$$\begin{aligned} A_1(^1S_0) &= \langle ^1S_0 | V_C G V_C | ^1S_0 \rangle =: A_{1\text{sym}}^{(S)} \\ A_1(^3S_1) &= \begin{pmatrix} |^3S_1\rangle \\ 0 \end{pmatrix}^\dagger \begin{pmatrix} V_C & \sqrt{8} V_T \\ \sqrt{8} V_T & V_C - 2V_T \end{pmatrix} G \begin{pmatrix} V_C & \sqrt{8} V_T \\ \sqrt{8} V_T & V_C - 2V_T \end{pmatrix} \begin{pmatrix} |^3S_1\rangle \\ 0 \end{pmatrix} \\ &= A_1(^1S_0) + \langle ^3S_1 | 8V_T G V_T | ^3S_1 \rangle =: A_{1\text{sym}}^{(S)} + A_{1\text{break}}^{(S)} \end{aligned} \quad (2.30)$$

The LO two-nucleon propagator G is Wigner-symmetric by virtue of the Unitarity Expansion. The breaking comes exclusively from once iterating the SD matrix element of the one-pion interaction. After all, $^3\text{SD}_1$ is a mixed channel, while 1S_0 is not. This symbolic notation does of course not imply as square of the incoherent SD transition amplitude $|\langle ^3S_1 | V_T | ^3D_1 \rangle|^2$. By Cutcosky's rule, this gives merely the imaginary part of on-shell propagation in the intermediate state. The real part is the off-shell contribution of the $S \rightarrow D \rightarrow S$ process. Finally, a DD matrix element does not appear before twice-iterated OPE, *i.e.* at $N^3\text{LO}$. To extend these arguments to other channels is straightforward [83].

We reiterate that this reasoning only applies to the pion-part of the interaction and the part of the corresponding CTs which absorbs cutoff-dependence for renormalisation. In our case, the “finite parts” of the corresponding LECs are determined by the empirical scattering lengths and effective ranges. These break Wigner-SU(4) symmetry explicitly but weakly. On the other hand, the distinction between Wigner-symmetric and breaking contributions holds for all regulators which preserve Wigner-SU(4) symmetry, like in the scheme we used: dimensional regularisation with Power-Divergence Subtraction [51, 52].

2.4.2 Pathway and Parameters

$$\begin{aligned}
\text{LO: } & \text{Diagram 1} = \text{Diagram 2} + \text{Diagram 3} + \text{Diagram 4} + \dots \\
\text{NLO: } & \left(\text{Diagram 5} + \text{Diagram 6} \right) \otimes \left(\text{Diagram 7} + \text{Diagram 8} \right) \otimes \left(\text{Diagram 9} + \text{Diagram 10} \right) \\
\text{N}^2\text{LO: } & \left(\text{Diagram 5} + \text{Diagram 6} \right) \otimes \left[\left(\text{Diagram 7} + \text{Diagram 8} \right) \otimes \text{Diagram 11} \otimes \left(\text{Diagram 7} + \text{Diagram 8} \right) + \text{Diagram 12} + \text{Diagram 13} + \text{Diagram 14} \right] \otimes \left(\text{Diagram 9} + \text{Diagram 10} \right)
\end{aligned}$$

Figure 2: (Colour on-line) $\chi\text{EFT}(\text{p}\pi)_{\text{UE}}$ at LO (top); NLO (middle) with CTs (red circle) fixed to reproduce scattering length a and effective range r ; N²LO with CTs (blue diamonds) fixed so that a and r do not change from the NLO value). The last term in square brackets at N²LO is once-iterated OPE.

We start with the NN amplitudes in the $^1\text{S}_0$ and coupled $^3\text{SD}_1$ channels with perturbative (KSW) pions. They were derived for finite scattering length by Kaplan, Savage and Wise [51, 52] to NLO, and extended to N²LO by Fleming, Mehen and Stewart [53, 54]. Indeed, the $^1\text{S}_0$ wave was first reported by Rupak and Shores (1S₀) [62] but does not differ from FMS. Figure 2 shows the $^1\text{S}_0$ and $^3\text{S}_1$ contributions at each order. The last line includes those diagrams with SD-mixing interactions, all of which enter only at N²LO. Those which enter only in the phase shift of the $^3\text{D}_1$ channel and of the SD mixing angle are discussed in an MSc thesis [63] and will be subject of a future publication [83]. In order to confirm that all are coded correctly, we checked that we reproduce the FMS results with their parameter values. This is nontrivial since some are highly sensitive to the exact numbers used³.

We then expanded them about Unitarity and determined the LECs at the natural renormalisation point of Unitarity, $k_{\text{fit}} = 0$. LO is Unitarity; NLO adds a finite scattering length, effective range and OPE; and N²LO adds corrections in a, r , and once-iterated OPE.

In contradistinction, FMS do not expand around Unitarity but find the LO LECs (equivalent to our fixing a) from the pole position in the amplitudes. Their dimensionless NLO and N²LO LECs ζ_1 to ζ_4 are determined by weighted least-squares fits to the Nijmegen PWA which do not change the LO pole positions. We did confirm FMS' finding that further coefficients ζ_5 and ζ_6 which parametrise the impact of higher-order contributions do not solve the poor convergence issues at N²LO and discard them here from the start.

For clarity, we regrouped the amplitudes into Wigner-SU(4) symmetric and breaking parts, each sorted by powers of the dimensionless ratio $\frac{k}{m_\pi}$. The results appear considerably shorter than those of FMS [53] for three reasons. First, they are rewritten using the ERE parameters a, r in favour of FMS' ζ_1 to ζ_4 . Second, the Unitarity Expansion leads to a few simplifications. Third, we found some more economical ways to rewrite certain terms.

³We are grateful for Iain Stewart's help in numerous conversations, both electronically and in person.

On a technical note, we do not differentiate between NN CTs which explicitly break chiral symmetry by quark (and hence pion) mass dependence. At NLO, a NN LEC $D_2 m_\pi^2$ enters [84] with the same operator structure as the CT whose LEC is determined by the scattering length. We do here not vary the pion mass, and the amplitudes we use are regulator-independent, so such effects cannot be disentangled.

We use the average nucleon and pion masses $M = 938.91897$ MeV, $m_\pi := \frac{2m_\pi^\pm + m_\pi^0}{3} = 138.037$ MeV, the axial pion-nucleon coupling $g_A = 1.267$, pion decay constant⁴ $f_\pi = 92.42$ MeV, and 197.327 fmMeV = 1. The position of cuts and poles in amplitudes induced by pionic effects is manifest for $m_\pi^2 \rightarrow m_\pi^2 - i\epsilon$ with $\epsilon \searrow 0$.

For the scattering lengths and effective ranges, we choose the values reported by the Granada group [23]: in the 1S_0 channel $a(^1S_0) = -23.735(6)$ fm and $r(^1S_0) = 2.673(9)$ fm; and in the 3S_1 channel $a(^3S_1) = 5.435(2)$ fm and $r(^3S_1) = 1.852(2)$ fm. The slightly different results and parameter values in the MSc thesis [63] used the Nijmegen group's 1995 analysis [20, 85]: $a(^1S_0) = -23.714$ fm and $r(^1S_0) = 2.73$ fm; $a(^3S_1) = 5.420(1)$ fm and $r(^3S_1) = 1.753(2)$ fm. However, differences in our NLO and N²LO results even at $k \approx 300$ MeV are smaller than 2.7° and hardly exceed the line widths. We discuss in sect. 3.6 how the amplitudes are modified for different fit points $k_{\text{fit}} \neq 0$.

A generic scattering length and effective range is in the following denoted by a and r . They are to be replaced by the values for the 1S_0 or 3S_1 channel as appropriate.

2.4.3 Amplitude at $\mathcal{O}(Q^{-1})$ (Leading Order)

The LO contribution at Unitarity is identical in the 3SD_1 and 1S_0 channel and therefore obviously both scale and Wigner-SU(4) invariant. Only the S-wave component is nonzero and of course identical to the pionless result of eq. (2.3):

$$A_{-1}^{(S)}(k) = \frac{4\pi i}{M} \frac{1}{k} . \quad (2.31)$$

2.4.4 Amplitude at $\mathcal{O}(Q^0)$ (Next-To-Leading Order)

Now, scattering length, effective range and pions enter:

$$A_0^{(S)}(k) = -\frac{4\pi}{Mk} \left(\frac{1}{ka} - \frac{kr}{2} \right) - \frac{g_A^2}{4f_\pi^2} \left(1 - \frac{m_\pi^2}{4k^2} \ln[1 + \frac{4k^2}{m_\pi^2}] \right) . \quad (2.32)$$

The first term is, as expected, the NLO amplitude of the pionless version, eq. (2.3). Thus, scattering length and effective range induce the *only* Wigner-SU(4) breaking effects at this order. While the pionic potential of eq. (1.4) breaks scale invariance and Wigner symmetry, its projections onto the 1S_0 and 3S_1 channels are identical as expected from the discussion in sect. 2.4.1. It is also the only non-analytic contribution, with just one branch point at $k = \pm i \frac{m_\pi}{2}$ from OPE. Therefore, χ EFT with Perturbative Pions at NLO naturally accommodates

⁴KSW and FMS use $f = \sqrt{2}f_\pi$ [51–54].

Wigner-SU(4) symmetry. At low momenta, the impact of $A_0^{(S)}(k)$ reduces to:

$$\lim_{k \rightarrow 0} k \cot \delta_{0,0}(k) = \left(-\frac{1}{a} + \frac{r}{2} k^2 \right) - \frac{g_A^2 M}{8\pi f_\pi^2 m_\pi^2} k^4 \left(1 + \mathcal{O}\left(\frac{k^2}{m_\pi^2}\right) \right) . \quad (2.33)$$

The non-pionic part is exactly the EFT($\not{\pi}$) result. Corrections come exclusively from pions and vanish at a dimensionless scale set by $\frac{g_A^2 M k^3}{8\pi f_\pi^2 m_\pi^2}$. Thus, they contribute substantially only for $k \gtrsim 100$ MeV: Pion contributions violate scale invariance only weakly for low momenta, and not at all for zero momenta. This is expected since we subsumed all scale breaking at $k = 0$ into the different scattering lengths and effective ranges in 1S_0 and 3S_1 . The $\mathcal{O}(g_A^2)$ contribution in eq. (2.32) constitutes only the long-range part of OPE (without iteration), after CTs absorb divergences to reproduce the empirical a, r . The phrase “pion contribution” is understood in that sense: the pionic long-distance part after renormalisation within the chosen renormalisation scheme (Power Divergence Subtraction in dimensional regularisation[51, 52]) and renormalisation condition ($k_{\text{fit}} = 0$ with empirical a and r).

Comparing NLO and LO, $A_0^{(S)}$ is indeed suppressed in the Unitarity Window ($\frac{1}{ka}, \frac{kr}{2} < 1$) if also $\frac{k}{\Lambda_{\text{NN}}} < 1$, *i.e.* if OPE is smaller than LO, consistent with the power counting.

2.4.5 Amplitude at $\mathcal{O}(Q^1)$ (Next-To-Next-To-Leading Order)

No new low-energy scattering parameters enter. As argued in the Introduction and sect. 2.4.1, the Wigner-SU(4) symmetric part of the amplitude is identical to the contribution in the 1S_0 channel which had already been found before FMS by Rupak and Shores [62]. We still call it “symmetric” or “invariant” albeit it does depend explicitly on a and r which break the symmetry if their values differ in the two channels:

$$\begin{aligned} A_1^{(^1S_0)}(k) \equiv A_{\text{1sym}}^{(S)}(k) &= \frac{\left[A_0^{(S)}(k) \right]^2}{A_{-1}^{(S)}(k)} + \frac{g_A^2}{2f_\pi^2} \left[\frac{4}{3am_\pi} - \frac{m_\pi}{k} \left(\frac{1}{ka} - \frac{kr}{2} \right) \right] \\ &\quad - \frac{g_A^2 M m_\pi}{16\pi f_\pi^2} \left\{ A_0^{(S)}(k) \frac{m_\pi}{k} \arctan\left[\frac{2k}{m_\pi}\right] + \frac{g_A^2}{2f_\pi^2} \left[\frac{1}{12} + \left(\frac{m_\pi^2}{4k^2} - \frac{1}{3} \right) \ln 2 - F_\pi\left(\frac{k}{m_\pi}\right) \right] \right\} . \end{aligned} \quad (2.34)$$

The first term combines the N²LO EFT($\not{\pi}$) amplitude of eq. (2.3) with insertions of the pionic NLO pieces; see eq. (2.32) and first term in square brackets in fig. 2. The second term is a correction from (non-iterated) OPE and CTs to keep a and r at N²LO fixed to the NLO values (N²LO diagrams labelled a, r and $\Delta a, \Delta r$ in fig. 2). The $\mathcal{O}(g_A^4)$ contributions (last line) encode the long-range part of once-iterated OPE via $S \rightarrow S \rightarrow S$ only (last N²LO diagram in square brackets of fig. 2 and eq. (2.30)). The amplitude has a branch point from non-iterated OPE at $k = \pm i \frac{m_\pi}{2}$, and in addition from once-iterated OPE at $k = \pm i m_\pi$. The latter comes from the last term of the dimensionless function

$$F_\pi(x) := \frac{1}{8x^3} \left(\arctan[2x] \ln[1 + 4x^2] - \text{Im} \left[\text{Li}_2\left[\frac{2ix + 1}{2ix - 1}\right] - 2\text{Li}_2\left[\frac{1}{2ix - 1}\right] \right] \right) \quad (2.35)$$

since Euler's Dilogarithm (Spence function) $\text{Li}_2(z) = -\int_0^z dt \frac{\ln[1-t]}{t}$ has a branch point at $z = 1$ [86, sect. 25.12(i)]. Furthermore, $F_\pi(x \rightarrow 0) = 1 - \frac{10x^2}{3} + \mathcal{O}(x^4)$ is finite as $k \rightarrow 0$, and $F_\pi(x \rightarrow \infty) = \frac{\pi}{8} \frac{\ln[2x]}{x^3} + \mathcal{O}(x^{-4})$ is its chiral limit.

For $g_A \rightarrow 0$, $A_1^{(1S_0)}(k)$ reduces to the pionless N²LO amplitude, eq. (2.3). Its contribution to $\text{kcot}\delta$ vanishes faster than k^2 , *i.e.* a and r are not shifted from the NLO values:

$$\lim_{k \rightarrow 0} \text{kcot}\delta_{1,0}(k)|_{\text{sym}} = \frac{g_A^2 M}{4\pi f_\pi^2 m_\pi} \left[\left(\frac{8}{5am_\pi^2} + \frac{r}{3} \right) - \frac{g_A^2 M}{4\pi f_\pi^2 m_\pi} \overbrace{\frac{(384 \ln 2 - 227)}{960}}^{=0.040800\dots} m_\pi \right] k^4 \left(1 + \mathcal{O}\left(\frac{k^2}{m_\pi^2}\right) \right) \quad (2.36)$$

has a one-pion contribution at dimensionless scale $\frac{g_A^2 M k^3}{4\pi f_\pi^2 m_\pi} (\frac{1}{am_\pi^2}, r)$ which is dominated by the size of $r \approx \frac{1}{m_\pi}$. When one uses $4\pi f_\pi \approx M$ and $\frac{g_A^2}{f_\pi} \approx r \approx \frac{1}{m_\pi}$, the scale for once-iterated OPE is of the same magnitude, $\frac{g_A^2 M k^3}{4\pi f_\pi^2 m_\pi^2}$. Both are hence again small for $k \lesssim m_\pi$.

A Wigner-SU(4) breaking part enters in 3S_1 amplitude [$F_\pi(x)$ has a different factor]:

$$A_1^{(3S_1)}(k) = A_{1\text{sym}}^{(S)}(k) + A_{1\text{break}}^{(S)}(k) \quad , \quad (2.37)$$

$$A_{1\text{break}}^{(S)}(k) = \frac{g_A^2}{f_\pi^2} \frac{g_A^2 M m_\pi}{16\pi f_\pi^2} \left\{ \overbrace{\frac{571 - 352 \ln 2}{210}}^{=1.5572\dots} - \left(1 + \frac{3m_\pi^2}{2k^2} + \frac{9m_\pi^4}{16k^4} \right) F_\pi\left(\frac{k}{m_\pi}\right) \right. \\ + \frac{2m_\pi^2}{5k^2} (\ln 4 - 1) + \frac{3m_\pi^4}{16k^4} - \frac{3}{2} \left[\left(\frac{k}{m_\pi} + \frac{m_\pi}{k} \right) - \left(\frac{m_\pi^3}{8k^3} + \frac{3m_\pi^5}{16k^5} \right) \right] \arctan\left[\frac{k}{m_\pi}\right] \\ \left. + \frac{3}{16} \left(\frac{m_\pi^4}{k^4} + \frac{3m_\pi^6}{4k^6} \right) \ln\left[\frac{16(k^2 + m_\pi^2)}{4k^2 + m_\pi^2}\right] \right\} - \frac{[A_0^{(\text{SD})}(k)]^2}{A_{-1}^{(S)}} \quad . \quad (2.38)$$

Since $A_{1\text{break}}^{(S)}$ is $\mathcal{O}(g_A^4)$, it comes exclusively from the transition $S \rightarrow D \rightarrow S$ of once-iterated OPE; see fig. 2 and $\langle ^3S_1 | 8V_T G V_T | ^3S_1 \rangle$ of eq. (2.30). It Wigner-SU(4) symmetry for lack of SD mixing in 1S_0 . All but the last part is the off-shell contribution. Branch points are again at $k = \pm i \frac{m_\pi}{2}$, $\pm i m_\pi$, with the latter from $\arctan \frac{k}{m_\pi}$, $\ln[k^2 + m_\pi^2]$ and F_π . The very last term is the on-shell piece, *i.e.* the NLO SD-mixing amplitude-squared

$$A_0^{(\text{SD})}(k) = -\frac{i g_A^2 m_\pi^2}{4\sqrt{2} f_\pi^2 k^2} \left[\frac{3m_\pi}{2k} - \left(1 + \frac{3m_\pi^2}{4k^2} \right) \arctan\left[\frac{2k}{m_\pi}\right] \right] \quad . \quad (2.39)$$

However, that term cancels the same contribution in the phase shift, eq. (2.8), and in $\text{kcot}\delta$, eq. (2.14), irrespective of whether $A_{-1}^{(S)}$ is at Unitarity or not. Since $A_0^{(\text{SD})}(k=0) = 0$, it does not contribute to shifting the pole, either; *cf.* eq. (2.22). The LO SD amplitude is zero; neither the N²LO nor any DD amplitude is needed for S-waves at the order we work [63, 83].

Finally, the symmetry-breaking part⁵ vanishes at low momenta again as $\frac{g_A^2 M k^3}{4\pi f_\pi^4}$, like the

⁵Since $A_0^{(S)}$ has no Wigner-SU(4) breaking contribution, $A_0^{(\text{SS})} = 0$ in eq. (2.14).

once-iterated symmetric OPE (using as before $4\pi f_\pi \approx M$ and $\frac{g_A^2}{f_\pi} \approx r \approx \frac{1}{m_\pi}$):

$$\lim_{k \rightarrow 0} \text{kcot}\delta_{1,0}(k)|_{\text{break}} = - \left(\frac{g_A^2 M}{4\pi f_\pi^2 m_\pi} \right)^2 \overbrace{\frac{384 \ln 2 - 187}{280}}^{=0.28274\dots} m_\pi k^4 \left(1 + \mathcal{O}\left(\frac{k^2}{m_\pi^2}\right) \right) . \quad (2.40)$$

As its contribution to $\text{kcot}\delta$ vanishes again like k^4 , a and r are not shifted from the NLO values. However, the term is about 5 times that of the Wigner-SU(4) symmetric part of once-iterated OPE, eq. (2.36). Both N²LO pieces are in the Unitarity Window suppressed against LO by powers of $Q \sim \frac{1}{ka}$, $\frac{kr}{2} < 1$, if also $Q \sim \frac{k, m_\pi}{\bar{\Lambda}_{\text{NN}}} < 1$. Indeed, the pionic N²LO pieces are roughly $\frac{k, m_\pi}{\bar{\Lambda}_{\text{NN}}} < 1$ relative to the pionic NLO contribution. This confirms Q and $\bar{\Lambda}_{\text{NN}}$ of eq. (1.5) as expansion parameter and breakdown scale of χEFT with Perturbative Pions [51] and the naïve dimensional estimate of once-iterated OPE in FMS [53].

3 Results and Analysis

For the reasons in sect. 2.2, we extract the phase shifts, pole positions and residues from amplitudes via $\text{kcot}\delta(k)$ using eqs. (2.12-2.14). The following plots contain the Bayesian truncation uncertainties at N²LO. These and other theory uncertainties will be discussed in sect. 3.5. All plots use the centre-of-mass momentum k as primary variable.

3.1 Zero-Momentum Limit and Pole Parameters

For $k \rightarrow 0$, all NLO and N²LO amplitudes contribute to $\text{kcot}\delta$ only via even powers of k , as required by analyticity below $k = |\pm i \frac{m_\pi}{2}|$ [67–70]. Since the renormalisation point is the ERE at $k = 0$ with Unitarity, $\frac{1}{a} = 0$, the LO contribution is $\text{kcot}\delta_{0,-1} = 0$. NLO in both $^1\text{S}_0$ and $^3\text{S}_1$ is $\text{kcot}\delta_{0,0} = \left(-\frac{1}{a} + \frac{r}{2}k^2\right) + \mathcal{O}(k^4)$; eq. (2.33). Both N²LO pieces vanish, $\text{kcot}\delta_{0,1} = 0 + \mathcal{O}(k^4)$; eqs. (2.36/2.40). Therefore, pole positions and residues are unchanged from the ERE/EFT(\not{x}) values of eqs. (2.26) to and (2.28) in sect. 2.3. As pointed out there, they match the empirical values within theory uncertainties.

3.2 The Spin Singlet, Isospin Triplet: $^1\text{S}_0$ Phase Shifts

The pionic contribution to the $^1\text{S}_0$ channel consists only of the Wigner-SU(4) invariant part. By inspection, its phase shift (top of fig. 3) converges well order-by-order until $k \rightarrow \bar{\Lambda}_{\text{NN}} \approx 300$ MeV approaches the putative breakdown scale. This point lies actually well outside the Unitarity Window (non-shaded area), but even there, the difference between N²LO and PWA is only as large as the difference between NLO and N²LO. Remarkably, N²LO is nearly indistinguishable from EFT(\not{x}) at NLO=N²LO. [Recall that its N²LO contribution to $\text{kcot}\delta$ is zero; see eq. (2.17).] Thus, explicit pionic degrees of freedom appear to have a minuscule impact even outside the formal radius of convergence of EFT(\not{x}), $k \gtrsim \frac{m_\pi}{2}$.

The Introduction identified the “physical part” of the amplitude, $\cot\delta$ in eq. (1.3), as the primary variable from which the phase shift can be found. Therefore, the bottom of fig. 3

also displays $\cot\delta$. Included are intervals around $N^2\text{LO}$ in which higher-order corrections should lie with 68% DoB, based on a Bayesian order-by-order convergence analysis under assumptions detailed in sect. 3.5.4. Section 3.5 will argue that this provides also a reasonable estimate of the smallest width of theory uncertainties combining several assessments.

The excellent agreement between PWA, $\text{EFT}(\pi)$ and $\chi\text{EFT}(\text{p}\pi)_{\text{UE}}$ at low k is a result of our fit to the ERE parameters. At high momenta, differences to the original results by Rupak and Shores, and by FMS [53, 62] are small. While our $N^2\text{LO}$ is above the PWA, theirs lies a bit below. We attribute this to two aspects: KSW fit at low k to the PWA,

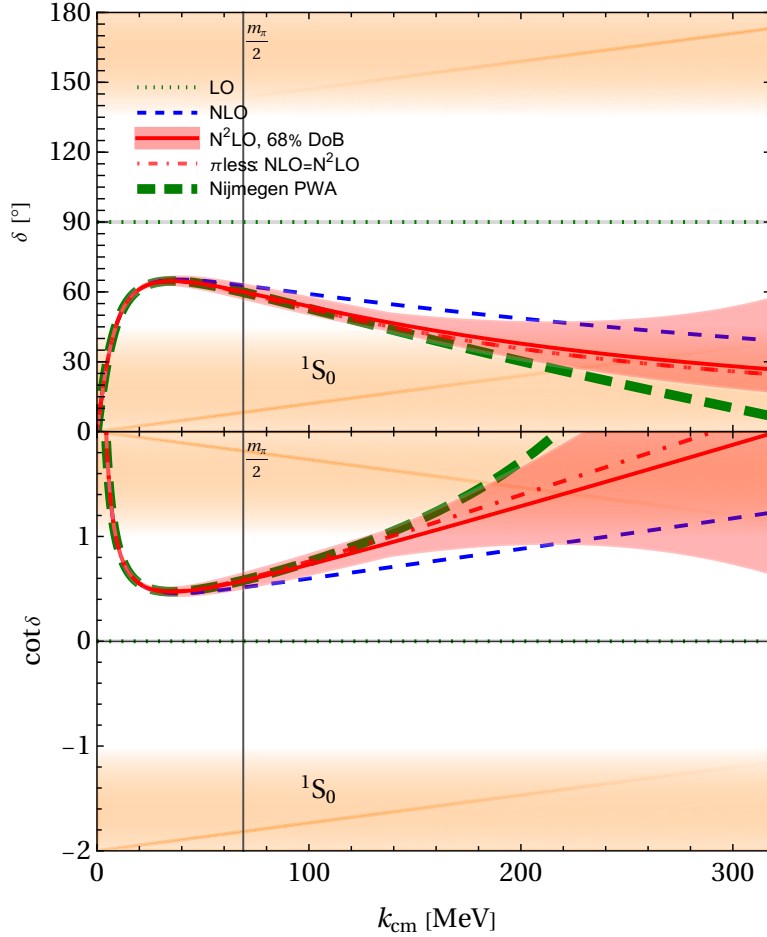


Figure 3: (Colour on-line) Phase shift (top) and $\cot\delta(k)$ in the 1S_0 channel as function of k , compared to the Nijmegen PWA [20] (thick green dashed). Green dotted: LO; blue dashed: NLO; red solid: $N^2\text{LO}$ with 68% degree-of-belief (DoB) interval based on the Bayesian truncation uncertainty under the assumptions of sect. 3.5.4; red dash-dotted: $\text{NLO}=\text{N}^2\text{LO}$ in $\text{EFT}(\pi)$. Shaded areas indicate the “Born Corridors” of fig. 1, *i.e.* regions in which the Unitarity Expansion can *a priori* not be expected to hold. Marked is also the scale of the first non-analyticity in $k\cot\delta(k)$, from the branch point $k = \pm i\frac{m_\pi}{2}$ of OPE.

while we use the ERE parameters; and we find phase shifts via $k\cot\delta$, while they determine δ directly using eqs. (2.6-2.8); see sect. 3.5.5. That we expand about Unitarity while they use a finite a at LO, has little impact since $\frac{1}{ka} \ll 1$ for large k .

In this channel, $\chi\text{EFT}(\pi\pi)_{\text{UE}}$ appears to overcome the conceptual issue that $\text{EFT}(\pi)$ is inapplicable above the first non-analyticity ($k = \pm i\frac{m_\pi}{2}$, OPE). It accomplishes the goal of a self-consistent theory with pions in all of the Unitarity Window.

3.3 The Spin Triplet, Isospin Singlet: 3S_1 Phase Shifts

Wigner-SU(4) breaking pion contributions enter at $\mathcal{O}(Q^1)$ (N^2LO). The result in fig. 4 is catastrophic, as FMS already noticed [53], with slight differences again because they extract phase shifts directly from the amplitudes. While NLO looks reasonable by eye, N^2LO deviates dramatically from the PWA just above the OPE branch-point scale of $\frac{m_\pi}{2}$.

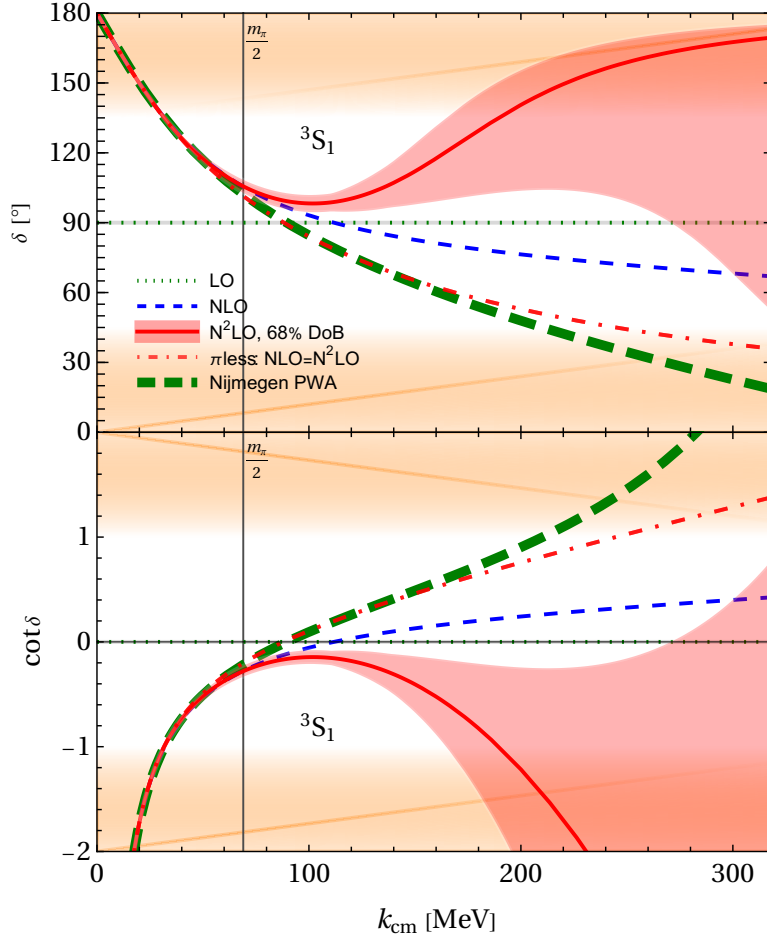


Figure 4: (Colour on-line) Phase shift (top) and $\cot\delta(k)$ (bottom) in the 3S_1 channel, compared to the Nijmegen PWA [20] (thick green dashed). Details as in fig. 3.

This is the more puzzling as $\text{EFT}(\pi)$ agrees well with the PWA albeit $k \gtrsim 100$ MeV is well outside its formal radius of convergence. With pions, the deviation between NLO and N^2LO becomes around $k \approx m_\pi$ as large as the difference between LO and NLO and larger than the deviation from the PWA. Not even the sign of $\cot\delta$ is correct. The breakdown is hardly gradual but sudden, with no hint at NLO of the unnaturally large N^2LO curvature around 100 MeV. This is the more concerning as phase shifts are there well inside the Unitarity Window. Pions at N^2LO appear to have an outsized and wrong impact for $k \gtrsim 100$ MeV.

In this channel, $\chi\text{EFT}(\text{p}\pi)_{\text{UE}}$ thus does not solve the conceptual issue that $\text{EFT}(\pi)$ is inapplicable above the nonanalyticity scale $\frac{m_\pi}{2}$. The radius of convergence is hardly extended. Most of the Unitarity Window lies outside it. That is unsatisfactory.

What is the origin of the stark discrepancy of both convergence and reasonable range of applicability between the $^1\text{S}_0$ and $^3\text{S}_1$ channels? The former is exclusively Wigner-SU(4) invariant; the latter has a symmetry-breaking component which according to sect. 2.4.1

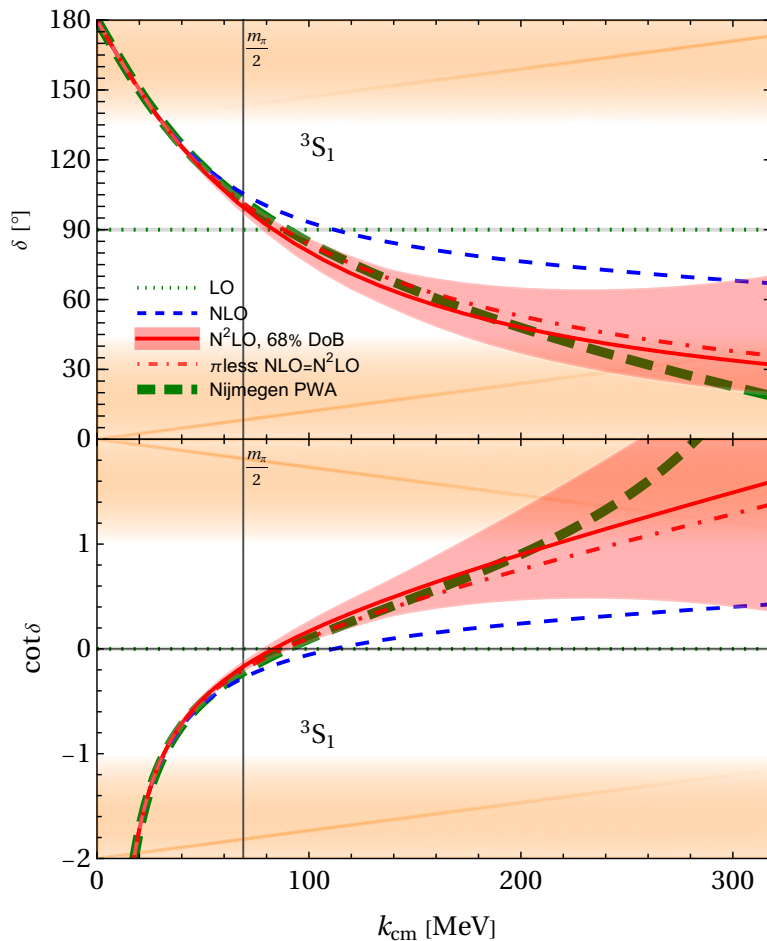


Figure 5: (Colour on-line) Phase shift (top) and $\cot\delta(k)$ (bottom) in the Wigner-symmetric $^3\text{S}_1$ channel, compared to the Nijmegen PWA [20] (thick green dashed). Details as in fig. 3.

comes exclusively from the tensor ($S \rightarrow D \rightarrow S$) part of once-iterated OPE. Mindful of the importance of this symmetry around Unitarity discussed in the Introduction, fig. 5 shows the 3S_1 channel without the Wigner-SU(4) symmetry-breaking term, eq. (2.38).

The qualitative and quantitative improvement is obvious. Similar to 1S_0 , the phase shift converges order-by-order even as $k \rightarrow \bar{\Lambda}_{\text{NN}} \approx 300$ MeV just outside the Unitarity Window. The difference between N²LO and PWA is wholly within the Bayesian 68% DoB band of sect. 3.5.4, even better than in the 1S_0 channel and quite a bit smaller than the shift from NLO to N²LO. Since $\chi\text{EFT}(\text{p}\pi)_{\text{UE}}$ at N²LO and $\text{EFT}(\not\pi)$ at NLO=N²LO are nearly indistinguishable, pionic degrees of freedom have again a minuscule impact even outside the formal convergence radius of $\text{EFT}(\not\pi)$, $k \gtrsim \frac{m_\pi}{2}$. Notwithstanding a detailed discussion in sect. 3.5, one can thus place the empirical breakdown scale of $\chi\text{EFT}(\text{p}\pi)_{\text{UE}}$ soundly around $k \gtrsim 250$ MeV or even 300 MeV.

We conclude that the Wigner-SU(4) invariant $\chi\text{EFT}(\text{p}\pi)_{\text{UE}}$ appears well-suited to overcome the conceptual inapplicability of $\text{EFT}(\not\pi)$ above the scale of the first branch point. In both the 1S_0 and 3S_1 channels, it is a self-consistent theory with pions in all of the Unitarity Window – and potentially somewhat beyond – with a common breakdown scale of at least $k \gtrsim 250$ MeV $\approx \bar{\Lambda}_{\text{NN}}$, plus good agreement with PWAs even at these high momenta.

3.4 Wigner-SU(4) Symmetric vs. Breaking Amplitude in 3S_1

Why do versions with and without Wigner-SU(4) symmetry-breaking terms lead to so different results? In contradistinction to $\text{EFT}(\not\pi)$, the pionic contributions to all amplitudes in χEFT with Perturbative Pions lead to nonzero coefficients of the ERE, and hence to predictions of all shape parameters v_n in (2.28); see eqs. (2.33), (2.36) and (2.40). Cohen and Hansen argued that PWA and FMS results diverge due to a “pattern of gross violation”: The coefficients v_n of the FMS ERE are too large by factors of at least 5 and usually 10 [87–89]. They showed that these are incompatible with the PWA values; see also the discussion in [90]. While the empirical values have changed since then [23], a stark discrepancy remains. To us, the reason appears to be that the v_n are actually much smaller than the naïve estimate $v_n \sim m_\pi^{-2n+1}$ suggests, while χEFT predicts usually coefficients of that size. Still, comparing phase shifts at NLO and N²LO with $\text{EFT}(\not\pi)$ in figs. 3 to 5 and sect. 3.4 shows that both theories describe the PWA analyses of both the 1S_0 and 3S_1 channel very well for $k \lesssim 70$ MeV, albeit $v_n \equiv 0$ in N²LO $\text{EFT}(\not\pi)$. This suggests that the *string* of v_n predictions in χEFT is highly correlated and produces *in toto* large cancellations between different v_n . This does not conflict with the χEFT power counting since, as discussed above, the contributions to *all* v_n are nonzero separately at *each* order of Q . The v_n may be vastly changing between orders, but their combined effect on the phase shifts (observables) does not. Eventually, a CT at $\mathcal{O}(Q^{2n-2})$ (N²ⁿ⁻¹LO) can be used to exactly match v_n to the empirical value, eliminating the issue up to that order and ERE coefficient altogether.

This can explain the agreement of the 1S_0 and Wigner-symmetric 3S_1 results with PWAs. Is it also key to the breakdown of the Wigner-breaking result? From eq. (2.36), the once-iterated, symmetry-breaking OPE which dominates as $k \rightarrow 0$ is $\propto k^4$ with a purely numerical coefficient of 0.28274 That is about a factor 7 bigger than the corresponding symmetric

coefficient $0.040800\dots$, eq. (2.40). The next terms, $\propto k^6$ etc., show a similar pattern. This could lead to subtle cancellations at low momenta which are overwhelmed at high k .

The top graph of fig. 6 compares the full amplitude to one in which one adds an expansion of $A_{1\text{break}}^{(S)}(k)$ up to $\mathcal{O}(k^{10})$ to the symmetric part, $A_{1\text{sym}}^{(S)}(k)$. [The series proceeds in powers of k^2 since the ERE is analytic [67–70].] If this converges, then it should smoothly interpolate between the Wigner-symmetric and full result as powers of k^2 are added.

However, large coefficients are clearly not the issue. Just as before, the symmetry-breaking portion is very small for $k \lesssim \frac{m_\pi}{2}$, the scale of the OPE branch point. Above it, the expansion does not converge at all. Each new term is bigger and alternates sign.

We therefore expanded also around $\frac{m_\pi}{2}$; all non-negative integer powers of k contribute. As discussed in sects. 2.4.4 and 2.4.5, contributions from this branch point appear at NLO and in both the symmetric and breaking terms of N²LO. According to the lower plot in fig. 6, this series interpolates well between symmetric and full amplitudes. Since the distance from

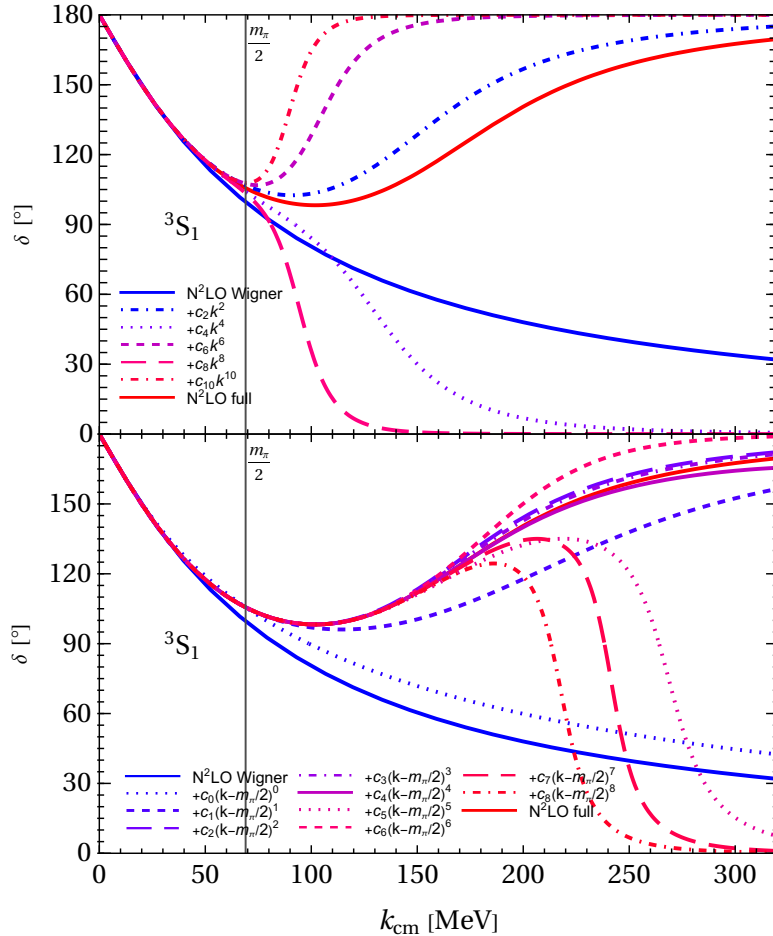


Figure 6: (Colour on-line) Interpolation between the Wigner-symmetric part and the full 3S_1 phase shift as expansion in powers of k ; see text for details.

the first branch point is increased, we find that convergence extends now indeed up to $k \approx \frac{m_\pi}{2} + \frac{m_\pi}{\sqrt{2}} \approx 170$ MeV. Above that, convergence is asymptotic with the best approximation to the full result when the 5th term, $\propto k^4$, is included – and this approximation is very good. We are unable to cast blame on any combination of terms in $A_{1\text{break}}^{(\text{S})}(k)$, eq. (2.38). We checked that Wigner-breaking terms with branch point at $k = \pm i m_\pi$ alone do not explain the big differences. Rather, the issue seems in combining all symmetry-breaking terms.

3.5 Assessing Uncertainties

In order to better quantify the preliminary conclusions, we turn to estimates of theory uncertainties: *a-priori* order-by-order convergence; *a-priori* estimates based on the assumption to be within the Unitarity Window; *data-driven* convergence to PWA results; *a-posteriori* order-by-order convergence via Bayesian statistics; and *a-posteriori* comparison of different ways to extract phase shifts. According to the “democratic principle”, different but reasonable choices should agree up to higher-order corrections. In concert, these therefore test to which degree various EFT assumptions are consistent with the outcomes. We disclose our choices and why believe they are reasonable to encourage discussion [61].

One test we cannot perform is insensitivity to variation of a cutoff scale which probes momenta beyond the range where the EFT applies; see *e.g.* [61, 91]. The amplitudes are analytically given using the physical scattering length and effective range to replace LECs at the renormalisation point $k = 0$ in the PDS scheme of dimensional regularisation [51, 52]. That choice eliminates any unphysical quantities.

3.5.1 A-Priori: Order-By-Order Estimates

The typical low-momentum scales are $\frac{1}{a} \rightarrow 0$ in the Unitarity Expansion, $r \sim \frac{1}{m_\pi}$, k and m_π . As discussed in sects. 2.4.4 and 2.4.5, n inverse powers of the *a-priori* breakdown scale $\bar{\Lambda}_{\text{NN}} \approx 300$ MeV parametrise the relative strength by which n -times-iterated OPE is suppressed against LO (no OPE). Therefore, $\frac{m_\pi}{\bar{\Lambda}_{\text{NN}}} \approx 0.5$ and for $Q \lesssim 1$ from eq. (1.5), the upper limit of χEFT with Perturbative Pions is expected to be $k \lesssim \bar{\Lambda}_{\text{NN}} \approx 300$ MeV.

Since $Q \approx 0.5$ at $k \approx m_\pi$ and results at N²LO are reported, corrections in $\cot\delta(k \sim m_\pi)$ should be of order $Q^3 \approx 0.1 = 10\%$, assuming the coefficients as of natural size [4, 60, 92–98]. At the high end, $k \rightarrow \bar{\Lambda}_{\text{NN}}$, NLO corrections and N²LO corrections should be of the same size ($\cot\delta = 0$ at LO does not set a scale). That happens at a slightly lower scale of $k \approx 150$ MeV in the ¹S₀ channel (*cf.* fig. 3). In the Wigner-symmetrised version of the ³S₁ wave, N²LO corrections are consistently somewhat larger than NLO, as allowed by naturalness, but they exceed thrice NLO at $k \approx 170$ MeV; fig. 5.

3.5.2 A-Priori: Inside the Unitarity Window

According to sect. 2.1, the Unitarity Window $\frac{1}{ka} < 1$ and $\frac{kr}{2} < 1$ imposes $8 \text{ MeV} \lesssim k \lesssim 140 \text{ MeV}$ in ¹S₀ and $35 \text{ MeV} \lesssim k \lesssim 200 \text{ MeV}$ in ³S₁. Ratios of small scales are not inconsistent with the Naturalness Assumption [4, 60, 92–98]: $|\frac{1}{am_\pi}| < 0.1$ in ¹S₀ and ≈ 0.25

in 3S_1 about Unitarity; $\frac{rm_\pi}{2} \approx 0.9$ in 1S_0 and ≈ 0.6 in 3S_1 . Therefore, changes from N³LO may at $k \approx m_\pi$ be $0.6^3 \approx 0.2$ in 3S_1 , and $0.9^3 \approx 0.7$ in 1S_0 — assuming again Naturalness. The latter is large, but NLO-to-N²LO corrections are actually smaller; see fig. 3.

3.5.3 Data-Driven: Convergence to the PWA

Comparison to an empirical PWA as next-best approximation to data can quantify how accurately the EFT reproduces experimental information [99, chap. 2.3] [100]. The double-logarithmic plots of fig. 7 contain information about expansion parameter and breakdown scale. First, deviations between calculation and data should be 1 for all orders when $Q \approx 1$. That determines the empirical breakdown scale $\bar{\Lambda}_{\text{emp}}$. Second, since each new order adds one power of $Q = \frac{k, m_\pi}{\bar{\Lambda}_{\text{emp}}}$ in the expansion of observables, slopes should increase by one power of Q from one order to the next in the range $k \gg m_\pi$ where the momentum scale dominates.

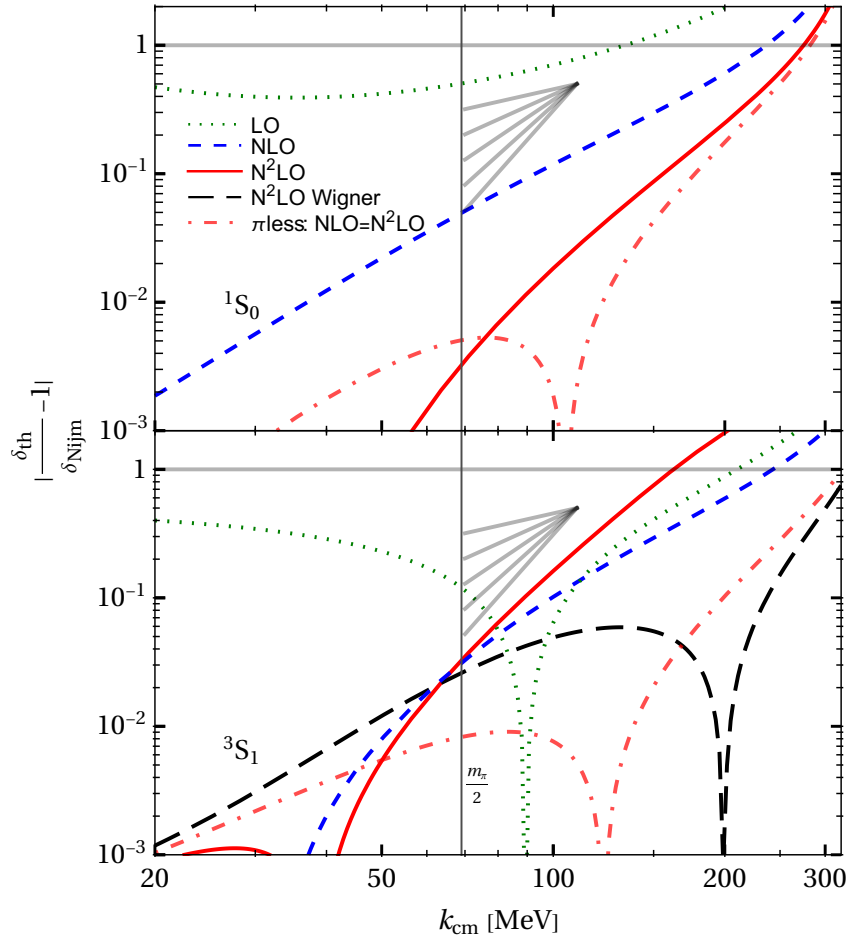


Figure 7: (Colour on-line) Double-logarithmic plots of the relative deviation between our results and the Nijmegen PWA in the 1S_0 (top) and 3S_1 (bottom) channels. The gray lines represent slopes of $k^{1,2,3,4,5}$. Colour-coding as in fig. 3.

Furthermore, the plots help quantify the assertions in sects. 3.2 and 3.3 that the Wigner-symmetric forms agree well with PWAs. Since the low- k phase shifts are fitted to the ERE which in turn is determined from a PWA, excellent agreement there is no surprise.

For the 1S_0 channel, NLO, N^2 LO and pionless corrections all approach unity around $\bar{\Lambda}_{\text{emp}}(^1S_0) \approx 270$ MeV which is close to the expected breakdown scale $\bar{\Lambda}_{\text{NN}} \approx 300$ MeV. We believe that is still sufficiently far away to be unaffected by the point $k \approx 350$ MeV where the Nijmegen PWA crosses zero but the $\chi\text{EFT}(\text{p}\pi)_{\text{UE}}$ result is nonzero. That induces an artificial divergence which cannot be remedied by plotting $\cot\delta$ instead. Slopes seem indeed to increase by roughly one from LO to NLO, and from NLO to N^2 LO, and N^2 LO is consistently more aligned with data than NLO. The $\text{EFT}(\pi)$ result might have an even better slope, but it suffers from an artificial zero since it crosses the empirical phase shift at an already relatively high $k \approx 100$ MeV. We estimate an empirical expansion parameter for momenta where the effects from reproducing the ERE has worn off. One reads off $Q(k \approx 200 \text{ MeV}) \approx 0.6$ from NLO, and $Q^2(k \approx 200 \text{ MeV}) \approx 0.25$ from N^2 LO. That is consistent with the *a-priori* estimate $Q = \frac{k \approx 200 \text{ MeV}}{\bar{\Lambda}_{\text{NN}}} \approx 0.7$, dropping the low scale m_π .

In the 3S_1 channel, the failure of the N^2 LO result including Wigner-breaking terms (red solid line) is obvious: It breaks down at $k \approx 150$ MeV. N^2 LO corrections are significantly larger than NLO ones for $k \gtrsim 100$ MeV. In contradistinction, the Wigner-symmetric version at N^2 LO (black long-dashed line) has the expected slope increase. For $k \gtrsim 170$ MeV, it demonstrates consistent improvement over NLO, towards the PWA, and, most remarkably, over $\text{EFT}(\pi)$. This adds to the evidence that $\chi\text{EFT}(\text{p}\pi)_{\text{UE}}$ has not only a radius of convergence which is formally larger than that of a pionless version, but also empirically. The extractions of an empirical breakdown scale at NLO (≈ 250 MeV) and N^2 LO (≈ 350 MeV) differ but are both well compatible with the expected breakdown scale $\bar{\Lambda}_{\text{NN}} \approx 300$ MeV. The issue may be that N^2 LO and PWA happen to agree at $k = 200$ MeV, inducing an artificial zero. That also makes it difficult to read off estimates of the expansion parameter for $k \gg m_\pi$. We find instead $Q(k \approx 120 \text{ MeV}) \approx 0.2$ from NLO, and $Q^2(k \approx 120 \text{ MeV}) \approx 0.06$ from N^2 LO, which is quite a bit smaller than an *a-priori* estimate $Q = \frac{(k \approx 120 \text{ MeV} + m_\pi)/2}{\bar{\Lambda}_{\text{NN}}} \approx 0.4$ in which m_π cannot be neglected as typical low scale.

3.5.4 *A-Posteriori*: Bayesian Order-By-Order Convergence

The *a-priori* estimates of sects. 3.5.1 and 3.5.2 can only qualitatively account for the Naturalness of coefficients [4, 60, 92–98]. Factors of 2 or 3 can change $\bar{\Lambda}_{\text{NN}}$ and order-by-order convergence substantially. A statistical interpretation via Bayesian analysis of the information on Naturalness that is available from the orders already calculated quantifies theory uncertainties from truncation at a given order; see *e.g.* [101–103] and references therein.

We first analyse truncation uncertainties for the pole position, eqs. (2.26) and (2.28), following the simple approach of refs. [79–81]. Expand

$$i\gamma = i \left[\gamma_{-1} + \gamma_0 + \sum_{n=1} \gamma_n \right] = i\gamma_0 \left[1 + \sum_{m=1} c_m \epsilon^m \right] \quad (3.1)$$

to define dimensionless coefficients c_m which are assumed to be of natural size, given an expansion parameter ϵ . For the pole position, eq. (2.26) suggests $\epsilon = \frac{r}{a}$, and consequently $c_1 = c_2 = \frac{1}{2}$. Since $i\gamma_{-1} = 0$ in the Unitarity Expansion, a scale is only set by $i\gamma_0 = \frac{i}{a}$. Truncated after n known coefficients, $|c_{\max, n+1}| \approx \max_{m \leq n} \{|c_m|\}$ reasonably estimates higher-order coefficients, so that $\pm |c_{\max, n+1}| \epsilon^{n+1}$ is a reasonable truncation uncertainty [78, sect. 4.4].

The BUQEYE collaboration showed how to derive probability distributions and degree-of-belief (DoB) intervals to statistically interpret $\pm |c_{n+1}| \epsilon^{n+1}$. A simple choice of priors is a uniform (flat) distribution for all known and unknown $|c_m|$ up to some (unknown but existing) maximum \bar{c} which follows a log-uniform distribution. With $n = 2$ terms known, $\pm |c_{\max, 3}| \epsilon^3$ encompasses roughly a 68% DoB interval. With only $n = 1$ term known, $\pm |c_{\max, 2}| \epsilon^2$ corresponds to a 50% DoB interval since fewer information leads to greater uncertainty. For these priors, the 68% DoB for $n = 1$ known term is actually at about $\pm 1.6 |c_{\max, 2}| \epsilon^2$, and the 95% interval for $n = 2$ known terms at about $\pm 2.7 |c_{\max, 3}| \epsilon^3$. This is not simply a factor 2 from the 68% DoB width for a Gaußian distribution because the posteriors fall off much slower, namely with inverse powers. Reasonable variations of the priors lead for $n \geq 2$ known drawings to variations by $\lesssim 20\%$ in these posteriors [80]. These are the 68% DoB intervals of the pole parameters in eq. (2.28).

We applied the same method to $\text{kcot}\delta(k)$ at each k and extracted the corresponding uncertainties for phase shifts. This assumes that uncertainties at different k are very strongly correlated, which appears reasonable given that $\cot\delta(k)$ is near-linear for $k \gtrsim 100$ MeV; *cf.* figs. 3 and 5. The LO coefficient is again zero, $\text{kcot}\delta_{0,-1} = 0$. We exploit that it is natural in the Unitarity Expansion to set the scale by the Unitarity-ensuring factor $-ik$ of the scattering amplitude, eq. (1.1)⁶. Since the theory is renormalised at $k = 0$ to reproduce the ERE, we ensure that uncertainty bands vanish as $k \rightarrow 0$ by setting

$$c_1 = \frac{\text{kcot}\delta_{0,0}(k) - \text{kcot}\delta_{0,0}(0)}{k Q} \quad , \quad c_2 = \frac{\text{kcot}\delta_{0,1}(k)}{k Q^2} \quad . \quad (3.2)$$

This choice is aligned with $\cot\delta$ as prime variable. We simply accommodate the various scales which make up the numerator of the expansion parameter in eq. (1.5) as

$$Q \approx \frac{\max\{k; m_\pi\}}{\bar{\Lambda}_{\text{NN}}} \quad , \quad (3.3)$$

noting that this choice of breakdown scale is consistent with the numbers in sect. 3.5.3. For NLO uncertainties, we rescale as above to find 68% DoB intervals.

The N²LO uncertainties are shown in figs. 3 to 5. Figure 8 shows them with the NLO bands (rescaled to 68% DoB). They overlap very well in the $^1\text{S}_0$ channel and reasonably in the Wigner-symmetric $^3\text{S}_1$ version. For both, the N²LO band is throughout smaller than the NLO one. In the $^3\text{S}_1$ wave with Wigner-breaking terms, NLO and N²LO uncertainties still overlap. However, the width of the N²LO band approaches that of NLO and grows even bigger for $k \gtrsim 250$ MeV, which is further proof that this version does not converge well.

⁶We thank D. R. Phillips for this suggestion.

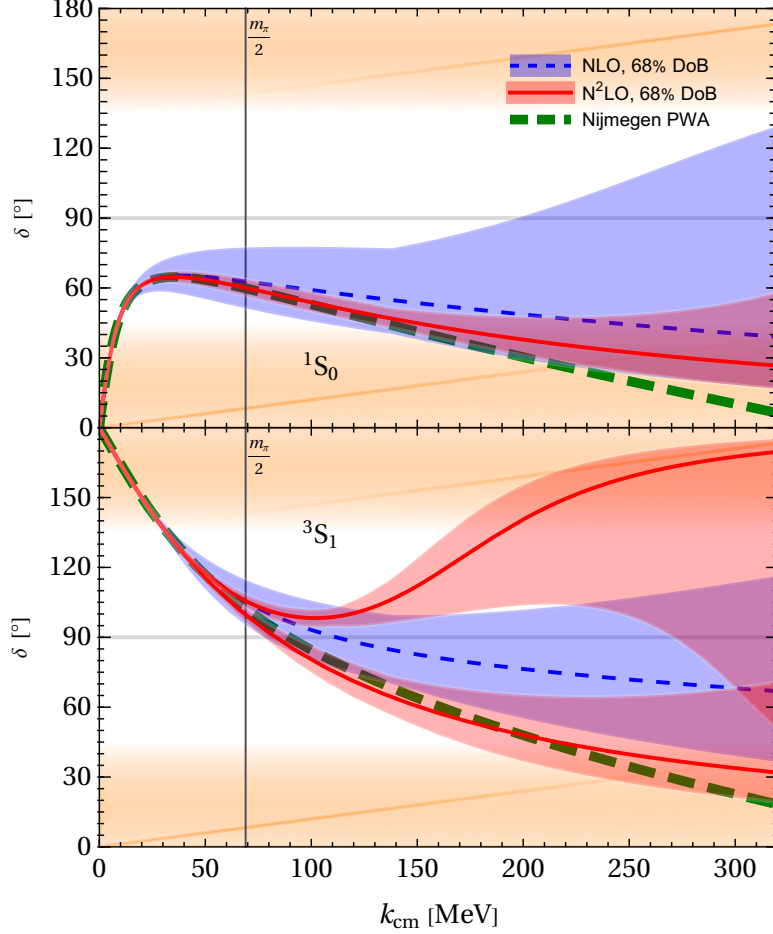


Figure 8: (Colour on-line) The 68% DoB uncertainties of phase shifts at N²LO (red) and NLO (blue, using the rescaling factor from 50% described in the text) in the ¹S₀ channel (top), and in the ³S₁ channel with and without Wigner-breaking terms (bottom), under the assumptions of priors described in the text. Details as in fig. 3.

Bayesian uncertainty estimations based on the factual convergence pattern of observables complement and do not replace conceptual arguments. If an expansion breaks for example down because nonanalyticities limit its radius of convergence, then an order-by-order assessment may be able to heuristically extend the range of applicability beyond that for some processes. But there is no reason why this should hold in all cases. If an EFT is not self-consistently renormalisable order-by-order, no statistical analysis can validate it.

3.5.5 *A-Posteriori*: Different Ways to Extract Phase Shifts

In sect. 2.2, we discussed two variants to extract phase shifts from amplitudes: directly, or via $k \cot \delta$. As noted there, when both are performed at the same order in Q , these two must agree up to higher-order corrections. If the results differ vastly, the expansion breaks down.

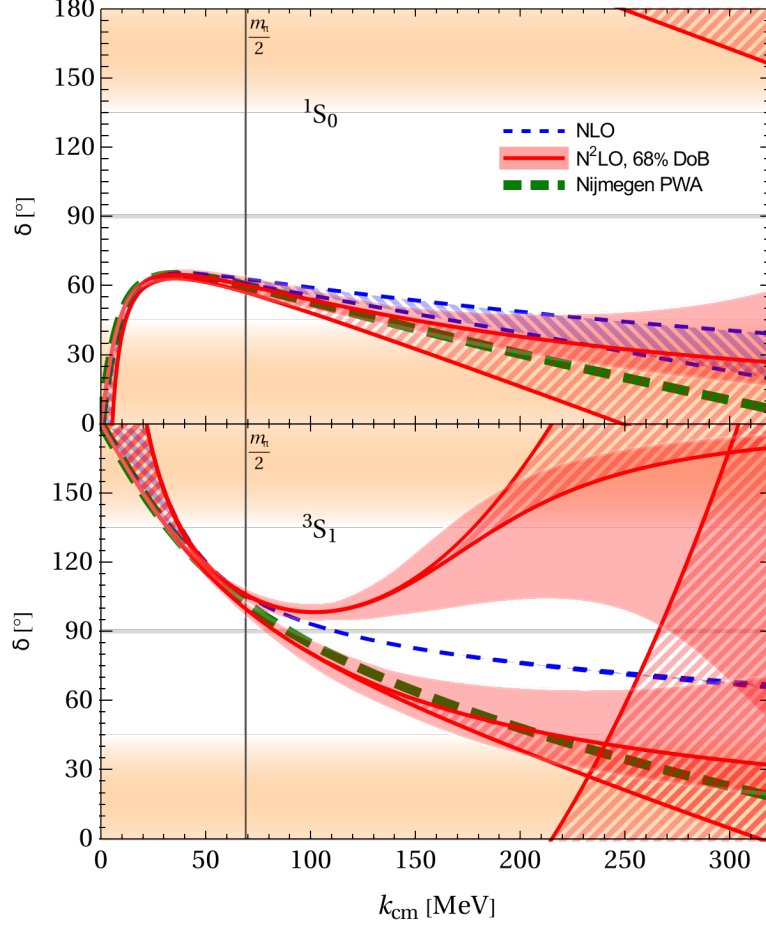


Figure 9: (Colour on-line) Phase shifts for the two variants to extract the 1S_0 (top) and 3S_1 (bottom) phase shifts of sect. 2.2: directly (pure lines), and via $k\cot\delta$ (lines with Bayesian uncertainty bands), at N²LO (red) and NLO (blue). The differences are marked by the hatched areas (blue: NLO; red: N²LO). Details as in fig. 3.

This is a particularly interesting tool to measure the size of the Unitarity Window. When one expands about its centre at $\cot\delta = 0$,

$$\cot\delta(k) = \left(\frac{\pi}{2} - \delta(k)\right) + \frac{1}{3} \left(\frac{\pi}{2} - \delta(k)\right)^3 + \mathcal{O}\left(\left(\frac{\pi}{2} - \delta(k)\right)^5\right) \quad (3.4)$$

proceeds in odd powers of $90^\circ - \delta(k)$. The first correction is smaller than $\frac{1}{4}$ of the leading term for approximately $\delta \in [40^\circ; 140^\circ]$, *i.e.* close to the points $\delta = 45^\circ, 135^\circ$ at which the Unitarity Expansion of eq. (1.3) is expected to fail because $|\cot\delta| = 1$.

It is therefore no surprise that figure 9 shows very good agreement between the extractions both at NLO and N²LO in all $\chi\text{EFT}(\text{p}\pi)_{\text{UE}}$ variants. At the low end of the Unitarity Window, the extractions diverge starkly for the reason discussed in sect. 2.2: According to eq.(2.16), using $k\cot\delta(k \rightarrow 0)$ leads to $\delta(k \rightarrow 0) = 0, 180^\circ$ at Unitarity from NLO on,

while the phase-shift extraction encounters a divergence, $\delta(k \rightarrow 0) \rightarrow \frac{1}{ka} \rightarrow \infty$, eq. (2.10). Discrepancies are therefore expected for $k \lesssim \frac{1}{|a|} = 8$ MeV in 1S_0 and $\lesssim 35$ MeV in 3S_1 . Interestingly, for higher momenta pushing into the Born Corridors, the induced bands become even smaller than the Bayesian uncertainty estimates, and phase shifts from the direct methods tend to lie slightly below the $k\cot\delta$ variant.

3.5.6 Summary and Conclusions: Theory Uncertainties

The *a-priori* estimates based on the expansion parameter Q of $\chi\text{EFT}(\text{p}\pi)_{\text{UE}}$ were refined by *a-posteriori* estimates, and supplemented further by data-driven convergence to the PWA. Since all these test complementing aspects, their uncertainties should be combined, but it is not clear how, and how uncorrelated these approaches are. Overall, all 5 findings are consistent with a breakdown scale of $\bar{\Lambda}_{\text{NN}} \approx 300$ MeV; a lower bound of the Unitarity Window of $k_{\text{low}} \lesssim 8$ MeV in 1S_0 and 35 MeV in 3S_1 ; and an expansion in Q as in eq. (1.5). The Bayesian uncertainty bands at N²LO appear to be a good estimate of truncation errors at about the 70% DoB level, possibly extending to slightly smaller phase shifts at given k .

3.6 Varying the Renormalisation Point

Another assessment of EFT uncertainties varies the renormalisation point, *i.e.* the input determining the LECs. So far, we used the ERE around $k = 0$ because that is the natural scale at Unitarity. Now, we treat the symbols a and r as if they were not scattering length and effective range but (finite pieces of) LECs whose values reproduce the Nijmegen values of $k\cot\delta$ and its derivative at a particular k_{fit} . Any choice is legitimate, as long as $k_{\text{fit}} \ll \bar{\Lambda}_{\text{NN}}$ [61]. In χEFT , a preferred “Goldilocks corridor” $k_{\text{fit}} \sim p_{\text{typ}} \sim m_\pi$ captures the Physics

k_{fit}	1S_0			3S_1		
	a [fm]	r [fm]	$(\gamma$ [MeV], Z)	a [fm]	r [fm]	$(\gamma$ [MeV], Z)
empirical	−23.735(6)*	2.673(9)*	(−7.892, 0.9034)	5.435(2)*	1.852(2)*	(+47.7023 , 1.689)*
pole	−23.7104	2.7783		5.6128	2.3682	
NLO	−38.988	3.3270	(−4.86 , 0.925)	4.9310	2.4966	(+55. , 1.9)
$\frac{m_\pi}{2}$ N ² LO	−25.428	2.7281	(−7.34 , 0.910(2))	4.7768	2.4492	(+57(3). , 1.9(2))
sym.				5.4625	1.6124	(+43.0(5) , 1.42(4))
NLO	+ 9.2856	4.2285	(+28. , 1.8)	3.3442 ⚡	3.1886 ⚡	(+114. , 3.) ⚡
m_π N ² LO	+34.3335	2.8956	(+6.01 , 1.10)	1.8376 ⚡	3.3741 ⚡	(+387(330)., 7(9).) ⚡
sym.				4.5344	1.7006	(+54(1). , 1.5(1))

Table 1: Values of a, r interpreted as LECs to reproduce $k\cot\delta$ and its derivative at a certain k_{fit} . The empirical values are found from the Granada values [23] as described in sect. 2.3. An asterisk $*$ is input; a lightning bolt $\boldsymbol{\text{⚡}}$ indicates the result cannot converge because $r \gtrsim a$. For a, r , spurious precision is used because of some fine-tuning. N²LO uncertainties for pole position γ and residue Z are based on the uncertainty estimate of sect. 2.3. If none is given, it is smaller than the last quoted significant figure.

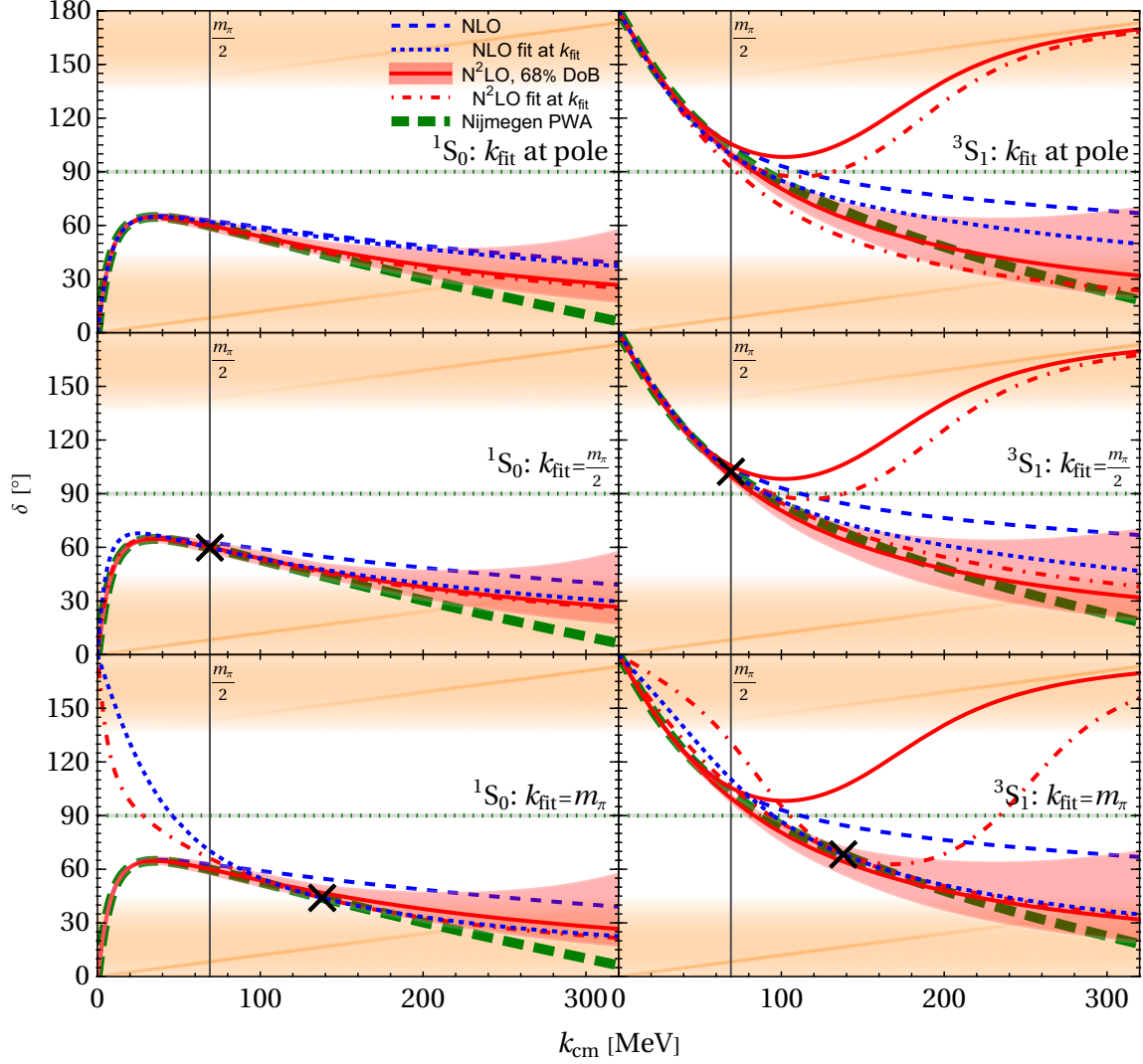


Figure 10: (Colour on-line) Phase shifts in the 1S_0 (left) and 3S_1 (right) channels, fitted to the pole (top), $k_{\text{fit}} = \frac{m_\pi}{2}$ (centre) and m_π (bottom). NLO: blue short-dashed. N²LO and Wigner-invariant N²LO are both red dot-dashed but simple to differentiate. Crosses mark fit points. The results for $k_{\text{fit}} = 0$ with Bayesian N²LO (in 3S_1 for the symmetric form only) bands are colour-coded as in fig. 3.

at the scales the EFT is designed for and helps avoid potential fine-tuning of coefficients between different orders. Such alternative determinations add another “uncertainty band” and test the stability of observables, expansion parameter and breakdown scale: The Callan-Symanzik renormalisation group equation’s variation of the renormalisation condition needs to be fulfilled up to higher-orders in the EFT expansion, wherever the EFT converges.

Rupak and Shores as well as FMS used the pole position of the amplitude as input [53, 62]. This natural choice for bound-state properties avoids trivial correlations

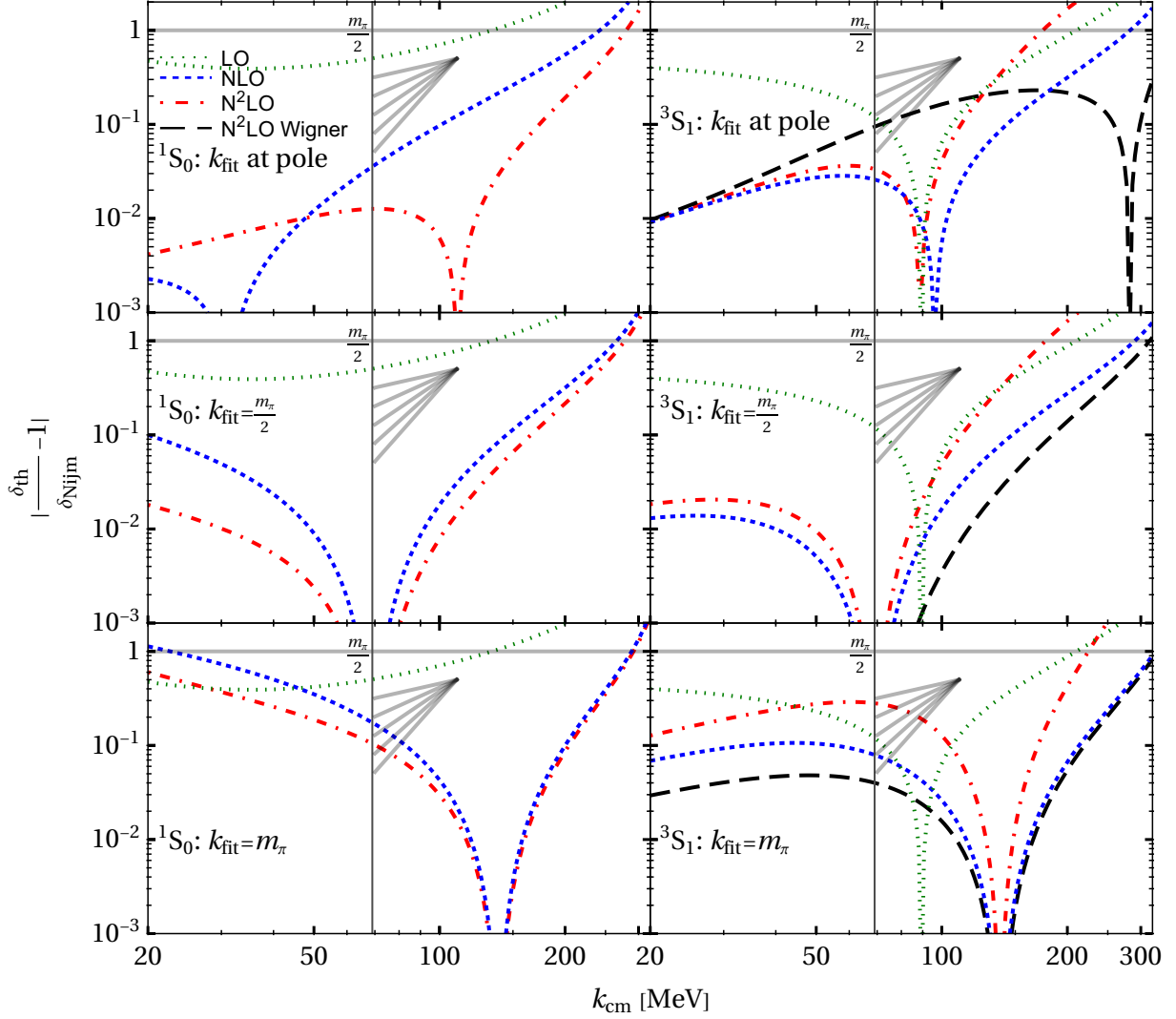


Figure 11: (Colour on-line) Double-logarithmic plots in the 1S_0 (left) and 3S_1 (right) channels of the relative deviation of results fitted to the pole (top), $k_{\text{fit}} = \frac{m_\pi}{2}$ (centre) and m_π (bottom), to the Nijmegen PWA. LO: green dotted; NLO: blue short-dashed; $N^2\text{LO}$: red dot-dashed; Wigner-symmetric $N^2\text{LO}$: black dashed; see also fig. 7.

between binding energies and observables like the charge radius. One can find such a and r from the empirical pole position and residue of eq. (2.28) up to $\mathcal{O}(\frac{r^3}{a^3})$ by inverting eqs. (2.26/2.27). No pion contributions enter. The results in table 1 differ only slightly from the Granada group's best values for physical scattering length and effective range at $k = 0$. On the other hand, since the leading nonzero contribution (NLO) is $i\gamma_0 = \frac{i}{a}$ from eq. (2.21), $k_{\text{fit}}a = \gamma a \approx 1$ lies by design just at the brink of the Unitarity Window. That is dangerous.

We therefore also explore two more renormalisation points inside the Unitarity Window which are natural in $\chi\text{EFT}(\text{p}\pi)_{\text{UE}}$: $k_{\text{fit}} = \frac{m_\pi}{2}$ and m_π , at the branch-point scales of non-

and once-iterated OPE. That $\frac{m_\pi}{2}$ is also in the region where both the 1S_0 and 3S_1 channels are closest to Unitarity ($\delta_{-1} \approx \frac{\pi}{2}$), makes it conceptually attractive. Remember that $\chi\text{EFT}(\text{p}\pi)_{\text{UE}}$ is constructed to explore precisely this very region $p_{\text{typ}} \sim m_\pi$ around Unitarity.

Figure 10 shows the phase shifts for the three choices, and fig. 11 the double-logarithmic plots of convergence to the PWA. The results of both fits to the pole and $\frac{m_\pi}{2}$ are well within the N²LO bands of 68% DoB uncertainties from Bayesian truncation uncertainties with $k_{\text{fit}} = 0$. According to table 1, the pole position and residue is still captured adequately, though discrepancies increase and order-by-order convergence gets poorer for $k_{\text{fit}} = \frac{m_\pi}{2}$. The nominal 1S_0 scattering length changes sign for $k_{\text{fit}} = m_\pi$ (bottom panels), and the extracted pole parameters and their uncertainties are meaningless since the phase shifts clearly diverge from the PWA well inside the Unitarity Window for $k \lesssim 60$ MeV. The 3S_1 results at NLO and Wigner-symmetric N²LO have $\frac{r}{a} \gtrsim 1$ (marked by lightning bolts ⚡ in table). This does not only violate the expansion of pole and residue in powers of $\frac{r}{a}$ (eqs. (2.26/2.27)), but also the Unitarity-Window constraint $\frac{r}{2a} \ll 1$. Apparently, the “leverage arm” from the fit point to the lower bound of the Unitarity Window is too large.

Interestingly, NLO is for all fit points at least as good, and sometimes even better, than the $k_{\text{fit}} = 0$ answers. Some of this may be because the phase shift is simply required to go through the PWA result. However, the N²LO curves with Wigner-SU(4) symmetry do not show such a uniform trend. The convergence plots of fig. 11 are very similar to the $k_{\text{fit}} = 0$ case for the pole fit. Except for the pole fit, they are dominated by the enforced identity with the phase shifts and derivatives of the PWA at the fit points. This makes the slopes seem steeper. However, the empirical breakdown scale of all fits is unchanged and in the same range of around 300 MeV as before. We therefore consider this to be a robust result.

The only exception is, of course, the 3S_1 channel with Wigner-SU(4) breaking interactions (red dot-dashed lines). Even when the fit forces it to match the empirical value at $k_{\text{fit}} = m_\pi$, does it diverge quickly at higher k . We see no scenario in which these amplitudes can be made to reasonably agree with the PWA, or with the pole position and residue (table 1).

Different but reasonable choices of the renormalisation point at N²LO do therefore not change phase shifts or empirical breakdown scales in a statistically significant way.

4 Summary and Conclusions

We discussed Chiral Effective Field Theory with Perturbative/“KSW” Pions in the Unitarity Expansion ($\chi\text{EFT}(\text{p}\pi)_{\text{UE}}$) in the 1S_0 and 3SD_1 channels of the NN system at next-to-next-to leading order (N²LO), imposing this limit on amplitudes by Rupak and Shores [62], and by Fleming, Mehen and Stewart [53, 54]; the analytic results are given in sect. 2.4.

In this formulation, Unitarity itself constitutes LO. This is the nontrivial fixed point of the renormalisation group flow. Its only scale is the relative momentum k . The momentum $k = 0$ at which no scale exists at all is its natural renormalisation point, *i.e.* the natural choice at which the Low-Energy Coefficients (LECs) of the Counter Terms (CTs) absorbing short-range details are fitted. Two-nucleon systems are there not only invariant under scaling, but also under Wigner’s combined SU(4) transformations of spin and isospin.

Around Unitarity ($k \cot \delta = 0$, $\delta = \frac{\pi}{2}$) lies the Unitarity Window of momenta roughly in the régime $40 \text{ MeV} \lesssim k \lesssim 200 \text{ MeV}$ with phase shifts $45^\circ \lesssim \delta(k) \lesssim 135^\circ$ ($|\cot \delta| \lesssim 1$). These are most important for many low-energy properties of nuclei. Unitarity implies Universality: Details of the interactions are less important than that their impact is so big as to come close to the bounds set by probability conservation. What separates different universality classes is the symmetries imposed at Unitarity. We find this confirmed since $\chi\text{EFT}(\text{p}\pi)_{\text{UE}}$ is in this window not just consistent but very close to “pionless” EFT – explicit pionic degrees of freedom appear to be of little consequence since both share the same (approximate) symmetries at the nontrivial fixed point; see sects. 3.2 and 3.3 and our final thoughts below.

Indeed, this observation nicely aligns with the viewpoint of Information Theory: The high degree of symmetry at Unitarity implies that the mere existence of an anomalously small scattering length is important, but not its actual value. In $\chi\text{EFT}(\text{p}\pi)_{\text{UE}}$, that value is demoted to be of less impact, namely only on par with information from the effective range and non-iterated OPE. All these are important at NLO and suppressed by $Q \approx 0.5$ relative to LO. Once-iterated OPE is the only information which enters one order in Q higher still, with $\approx 25\%$ relevance, but is completely determined by LECs (*i.e.* short-range information) available already at NLO. This sheds new light on a central EFT promise about encoding the unresolved short-distance information: The high degree of symmetry at Unitarity leads to a better-optimised lossless compression of information, namely to a reduction of the number and relative importance of independent LECs which encode the information in NN scattering at given accuracy. The most important aspect of both EFT($\not{\pi}$) and $\chi\text{EFT}(\text{p}\pi)_{\text{UE}}$ is that they both encode as the most important information the existence of anomalously small intrinsic scales, so their results agree very well – everything else is detail.

In this χEFT , both Wigner-SU(4) and scaling invariance are weakly broken in a systematic expansion in small, dimensionless parameters: $Q \sim \frac{1}{ak}$ and $Q \sim \frac{rk}{2} \lesssim 1$ define the Unitarity Window; and $Q \sim \frac{p_{\text{typ}}}{\Lambda_{\text{NN}}} \lesssim 1$ the chiral expansion, with $p_{\text{typ}} \sim k, m_\pi$ typical low-momentum scales. We find that $\chi\text{EFT}(\text{p}\pi)_{\text{UE}}$ provides at N²LO a description of the Physics inside the Unitarity Window which is both conceptually fully consistent and convergent. Comparison to pole parameters and Partial Wave Analyses (PWAs), a Bayesian analysis of order-by-order convergence, plus variations of both extraction methods and the renormalisation point consistently show that the expansion parameter is consistent with the above *a-priori* estimates, and that its empirical breakdown scale is consistent with $\bar{\Lambda}_{\text{NN}} = \frac{16\pi f_\pi^2}{g_A^2 M} \approx 300 \text{ MeV}$. This is the scale where χEFT with Perturbative Pions is expected to become inapplicable because iterations of OPE are not suppressed; see sect. 3.5. Thus, $\chi\text{EFT}(\text{p}\pi)_{\text{UE}}$ appears to also apply somewhat into the Born Corridor $|\cot \delta| \gtrsim 1$. That is not surprising as the perturbative (Born) approximation for $\cot \delta \gtrsim 1$ and $\chi\text{EFT}(\text{p}\pi)_{\text{UE}}$ for $\cot \delta \lesssim 1$ must match in the transition region, $\cot \delta \approx 1$. In contradistinction to the Unitarity Expansion in EFT($\not{\pi}$), $\chi\text{EFT}(\text{p}\pi)_{\text{UE}}$ ’s formal radius of convergence is not limited by the scales associated with the branch points of non- and once-iterated OPE, $\frac{m_\pi}{2}$ and m_π .

However, $\chi\text{EFT}(\text{p}\pi)_{\text{UE}}$ converges in the $^3\text{S}_1$ channel only because it keeps just the central part of once-iterated OPE; see sects. 2.4.1, 3.3 and 3.4. Like the non-iterated OPE at NLO, it is automatically Wigner-SU(4) invariant. Traditional chiral power counting adds the

symmetry-breaking tensor part at N²LO for perturbative pions, but the phase shifts do then not converge order-by-order and dramatically disagree with the PWA for $k \gtrsim 100$ MeV. This is unsatisfactory since the 3S_1 phase shift is there actually very close to Unitarity, $\delta(^3S_1, k \approx 100 \text{ MeV}) \approx 85^\circ$. This would be a failure for a description which wants to merge Unitarity and chiral Physics with perturbative pions in all of the Unitarity Window. On the other hand, demoting Wigner-breaking effects for perturbative pions to enter not before N³LO leads to results which converge very well both order-by-order and to the PWA in all of the Unitarity Window. This evidence led us to hypothesise in the Introduction:

Hypothesis: The symmetries of the Unitarity limit are broken weakly in Nuclear Physics. Their footprint shows *persistence*, *i.e.* their impact dominates observables at momentum scales $p_{\text{typ}} \sim m_\pi$ and beyond, and is more relevant than chiral symmetry. In particular, the tensor/Wigner-SU(4) symmetry-breaking part of one-pion exchange in the NN 3S_1 channel is super-perturbative, *i.e.* does not enter before N³LO.

Our study considered only the Wigner-doublet formed by the 1S_0 and 3S_1 channels. Both are well inside the Unitarity Window. We did not address at which order the tensor/Wigner-SU(4) breaking part of one-pion exchange (OPE) enters – except that it is at least N³LO.

Only those channels are Wigner-SU(4) symmetric in which the tensor interaction V_T is identical zero, like 1S_0 and 1P_1 ; see sect. 2.4.1. The invariance is broken in amplitudes with at least one insertion of V_T , like in 3SD_1 and 3P_0 . It is natural to assume that the amount of breaking is exponentially proportional to the number of V_T insertions. However, the function $\text{kcot}\delta_l(k \rightarrow 0) \propto k^{-2l} \rightarrow \infty$ is well outside the Unitarity Window at low momenta in partial waves with orbital angular momentum⁷ $l \geq 1$. Few reach phase shifts $|\delta(k)| \gtrsim 10^\circ$ ($|\cot\delta| \lesssim 5$) and thus may even remotely tend into the Unitarity Window. Of these, only the following are not singlets under Wigner-SU(4) transformations [35]: a Wigner-quadruplet (SU(4) antisymmetric super-sextuplet Irrep $\mathbf{6}_A$) consisting of the spin-singlet isospin-triplet 1D_2 and the Wigner-symmetric components of the spin-triplet-isospin-singlets 3D_2 and 3DF_3 , as well as 3D_1 which we however prefer to count as part of the Wigner-doublet 1S_0 - 3SD_1 because of its mixing with the 3S_1 wave; and a Wigner-quadruplet consisting of the spin-singlet-isospin-singlet 1P_0 and the Wigner-symmetric components of the spin-triplet isospin-triplets 3P_0 - 3P_1 - 3PF_2 residing in a symmetric SU(4) super-decuplet Irrep $\mathbf{10}_S$, just like the Wigner-doublet 1S_0 - 3SD_1 . In each case, the central components V_C of the OPE potential in the Wigner-multiplet are identical, while the tensor/Wigner-breaking components V_T differ. In none does the magnitude of the phase shift exceed even 25° ($|\cot\delta| \approx 2$) for $k \lesssim 300$ MeV, so they are all quite likely outside the Unitarity Window. Still, one can explore in-how-far these are impacted by Wigner symmetry at Unitarity.

Returning to a point raised in the Introduction, the Unitarity Expansion may offer a resolution to the conflict between Wigner symmetry and the large- N_C expansion of QCD. In the latter, the leading non-tensor part of the NN interaction is automatically Wigner-SU(4) symmetric in partial waves with even orbital angular momentum [33, 34]. However, this only holds if the tensor (Wigner-breaking) interaction is neglected altogether, and does not apply

⁷A more careful K -matrix analysis of partial-wave mixing does not change this conclusion [63].

to odd partial waves. And yet, weakly broken Wigner symmetry is in conflict with the large- N_C finding that the tensor (Wigner-breaking) interaction should be a leading contribution of the NN interaction. Calle Cordón and Ruiz Arriola concisely summarised this quandary and proposed as solution that Wigner-SU(4) symmetry is realised in the intermediate- and long-range part of the interaction, but strongly broken at short distances [35].

Like Calle Cordón and Ruiz Arriola, we see evidence for a splitting of Wigner-breaking between medium/long- and short-range contributions. Recall from sect. 2.4.4 that the “pion contribution” is actually only the pionic long-distance part in the chosen renormalisation scheme and condition. By fitting to a, r , we lock long-range Wigner-breaking into the short-distance Counter Terms and guarantee that pion amplitudes must vanish at very long distances, $k \rightarrow 0$. While we found that the Wigner-breaking (tensor) interaction becomes strong in 3S_1 for intermediate distances (momenta $k \gtrsim 80$ MeV), leading to unacceptable convergence problems, we can again discard the offending term by invoking that the Unitarity Expansion’s Wigner symmetry should be broken weakly.

In this interpretation, the large- N_C argument that the tensor interaction dominates, only holds if its leading coefficient is actually of natural size. We propose that an additional symmetry not accounted for by only applying large- N_C is imposed, namely Wigner-SU(4) as result of the proximity to the Unitarity fixed point. This forces this very coefficient to be zero, resolving the apparent conflict between the two symmetries. In this context, the fact that Wigner symmetry is a fixed-point symmetry is particularly powerful since it virtually guarantees that it survives renormalisation as long as the renormalisation scheme itself respects the fixed-point symmetries. Clearly, this mechanism is as of yet mere speculation.

In our approach, imposing Wigner symmetry as principle is only legitimate for channels whose phase shifts are close to the Unitarity fixed point, *i.e.* for S waves only. Therefore, no contradiction exists between Wigner symmetry and large- N_C for any higher partial waves, simply because Wigner symmetry does not apply there. This also cures the problem that this symmetry is realised at best extremely poorly in higher partial waves. For example, there might be some semblance when comparing the $^3P_{0,3}$ waves, and separately for the $^{1,3}P_1$ waves, but definitely none between these pairs which do not even agree on the sign.

Such arguments focused on the size of the phase shift do not quite apply to the impact of Unitarity on 3SD_1 mixing and the 3D_1 wave since these are coupled with 3S_1 which clearly is within the Unitarity Window. Results on these will be presented in the future [83]. For these, all terms in the amplitude come from the tensor interaction V_T and therefore break Wigner-SU(4) symmetry, but the LO amplitude A_{-1}^S at Unitarity enters in phase shifts. The question is therefore to which extent a demotion of tensor-interactions as in the Hypothesis is found there. After all, both mixing angle ε and D-wave phase shift δ_2 are small. Imposing Wigner-SU(4) symmetry at N²LO means that mixing angle and D wave are nonzero at most as early as $\mathcal{O}(Q^2)$ (N³LO), so $\varepsilon, \delta_2 = 0 + \mathcal{O}(Q^2)$. With $Q \sim 0.5$ (0.9) at $k \approx m_\pi$ ($2m_\pi$) or so and LO being $\mathcal{O}(Q^{-1})$, their natural magnitude can *a priori* be estimated as $(0.5)^3 \lesssim 10^\circ$ ($(0.9)^3 \lesssim 40^\circ$). This is still bigger than but for a rough estimate not entirely incompatible with the actual values $\varepsilon(m_\pi) \approx 2^\circ$ ($\varepsilon(2m_\pi) \approx 3^\circ$), $\delta_2(m_\pi) \approx -5^\circ$ (-15°) and might indicate that V_T enters only at even higher orders. The Unitarity Expansion might thus naturally answer the question why both the SD mixing angle and D wave phase shift are so small; see

first results in ref. [63].

Further studies are clearly warranted. If the Hypothesis is to be successful, then a systematic expansion must be found with Wigner-SU(4) symmetry as guiding principle to decide both *a priori* and semi-quantitatively at which order Wigner-breaking pion contributions and correlated two-pion exchange enter. Large N_C might provide such a parameter. Equally importantly, the Hypothesis breaks chiral symmetry at N²LO in pion interactions between nucleons. One must find a reason why this violation is not that important. The Goldstone mechanism converting global chiral symmetry into local, weakly interacting field excitations may eventually be too strong to overcome and lead to the Hypothesis’ downfall.

On this issue, the renormalisation group may provide further insight. The fixed point at Unitarity has only two characteristics: it is non-Gaussian (LO is nonperturbative) in the two- and few-nucleon sector with nonrelativistic nucleonic degrees of freedom; and it has specific symmetries. By definition, Physics is there scale/conformally invariant. In Nuclear Physics, the universality class of the nontrivial fixed point is defined by adding invariance under Wigner-SU(4) transformations. Universality requires that all such theories agree at Unitarity. Chiral symmetry is unknown to EFT(π), the EFT of χ EFT very close to the fixed point (very-low momenta). It is therefore subdominant in the vicinity of the fixed point; Wigner-SU(4) symmetry and its weak breaking dominate. If this were not correct, then χ EFT would lie in a different universality class than EFT(π). The Unitarity fixed point protects Wigner-SU(4) symmetry to be only weakly broken, while chiral symmetry in the few-nucleon sector has no such strong protection, simply because it is not a characteristic symmetry of the fixed point. Such reasoning does not apply to the zero- and one-nucleon sector of χ EFT since the projection of the fixed point onto these is Gaussian, *i.e.* these sectors are perturbative at LO. The argument is plausible but needs to be studied quantitatively.

The Hypothesis should also be tested in systems with at least 3 nucleons and with external probes. Such studies can start from comparisons between data and χ EFT with Perturbative Pions at NLO (without Unitarity Expansion) in 2N and 3N systems, including external probes; see *e.g.* [76, 84, 104–107]. These should be extended by at least one order. Because of the issues with chiral symmetry, pion photoproduction and scattering may be of particular interest. Fortunately, computations become actually simpler in the Unitarity Expansion, as can be seen from comparing our amplitudes to the FMS results.

Clearly, the Unitarity Expansion should also be explored in the χ EFT version in which pions are nonperturbative. First LO results were reported in three presentations [66, 108, 109], and a publication is in preparation [110]. Both for perturbative and nonperturbative pions, further clarifications are needed. Can imposing a preference for Unitarity as a highly symmetric state about which to expand provide a quantitative answer to the question posed in the Introduction: why is fine-tuning preferred? How does varying m_π affect the conclusions? In-how-far is the Unitarity limit compatible with the chiral limit? We see our Hypothesis merely as a first proposal to merge two highly successful concepts of Nuclear Theory, namely the expansion about Unitarity and χ EFT, for mutual benefit and a better understanding of why fine-tuning emerges in low-energy Nuclear Physics.

Author Contributions

All authors shared equally in all tasks.

Data Availability Statement

All data underlying this work is available in full from the corresponding author upon request.

Code Availability Statement

MATHEMATICA notebooks are available in full from the corresponding author upon request.

Declarations of Competing Interests

The authors have no financial or non-financial competing interests deriving from personal or financial relationships with people or organisations which may cause them embarrassment.

Acknowledgements

This project was conceived thanks to the warm hospitality and financial support of Beihang University (Beijing, China) and of the workshop EFFECTIVE FIELD THEORIES AND AB INITIO CALCULATIONS OF NUCLEI in Nanjing (China). Feedback to presentations at the ECT* workshop THE NUCLEAR INTERACTION: POST-MODERN DEVELOPMENTS and at the 11TH INTERNATIONAL WORKSHOP ON CHIRAL DYNAMICS (CD2024) was incorporated. We gratefully acknowledge the organisers and participants of the programme and workshop INT-24-3 QUANTUM FEW- AND MANY-BODY SYSTEMS IN UNIVERSAL REGIMES at the Institute for Nuclear Theory of the University of Washington for critically evaluating these ideas during the completion of this work (INT-PUB-24-052). We are grateful to the organisers and participants of these meetings for a highly stimulating atmosphere, including Bingwei Long and Dean Lee for discussions. We are indebted to U. van Kolck for encouragement during the early stages and extensive discussions in the final stages. Ian Stewart clarified typographical errors in the KSW and FMS publications (some of which are fortunately not in the arXiv versions of [52–54]). Daniel R. Phillips’ and Roxanne P. Springer’ valuable suggestions and pointers to pertinent publications about the large- N_C limit as well as Mike Birse’s concise comments dramatically improved the first arXiv version. This work was supported in part by the US Department of Energy under contract DE-SC0015393, and by George Washington University: by the Office of the Vice President for Research and the Dean of the Columbian College of Arts and Sciences; by an Enhanced Faculty Travel Award of the Columbian College of Arts and Sciences. HWG’s research was conducted in part in GW’s Campus in the Closet.

References

- [1] E. Epelbaum, U. G. Meißner and W. Glöckle, Nucl. Phys. A **714** (2003), 535-574 doi:[10.1016/S0375-9474\(02\)01393-3](https://doi.org/10.1016/S0375-9474(02)01393-3) [[arXiv:nucl-th/0207089](#) [nucl-th]].
- [2] E. Braaten and H. W. Hammer, Phys. Rev. Lett. **91** (2003), 102002 doi:[10.1103/PhysRevLett.91.102002](https://doi.org/10.1103/PhysRevLett.91.102002) [[arXiv:nucl-th/0303038](#) [nucl-th]].
- [3] S. R. Beane, K. Orginos and M. J. Savage, Int. J. Mod. Phys. E **17** (2008), 1157-1218 doi:[10.1142/S0218301308010404](https://doi.org/10.1142/S0218301308010404) [[arXiv:0805.4629](#) [hep-lat]].
- [4] H.-W. Hammer, S. König and U. van Kolck, Rev. Mod. Phys. **92** (2020), no. 2, 025004 doi:[10.1103/RevModPhys.92.025004](https://doi.org/10.1103/RevModPhys.92.025004) [[arXiv:1906.12122](#) [nucl-th]].
- [5] R. Machleidt and F. Sammarruca, Prog. Part. Nucl. Phys. **137** (2024), 104117 doi:[10.1016/j.ppnp.2024.104117](https://doi.org/10.1016/j.ppnp.2024.104117) [[arXiv:2402.14032](#) [nucl-th]].
- [6] A. Kievsky and M. Gattobigio, Few Body Syst. **57** (2016), 217 doi:[10.1007/s00601-016-1049-5](https://doi.org/10.1007/s00601-016-1049-5) [[arXiv:1511.09184](#) [nucl-th]].
- [7] S. König, H. W. Griesshammer, H. W. Hammer and U. van Kolck, Phys. Rev. Lett. **118** (2017), no. 20, 202501 doi:[10.1103/PhysRevLett.118.202501](https://doi.org/10.1103/PhysRevLett.118.202501) [[arXiv:1607.04623](#) [nucl-th]].
- [8] U. van Kolck, Few Body Syst. **58** (2017), no. 3, 112 doi:[10.1007/s00601-017-1271-9](https://doi.org/10.1007/s00601-017-1271-9).
- [9] U. van Kolck, Nuovo Cim. C **42** (2019), no. 2-3-3, 52 doi:[10.1393/ncc/i2019-19052-7](https://doi.org/10.1393/ncc/i2019-19052-7)
- [10] S. König, Eur. Phys. J. A **56** (2020), no. 4, 113 doi:[10.1140/epja/s10050-020-00098-9](https://doi.org/10.1140/epja/s10050-020-00098-9) [[arXiv:1910.12627](#) [nucl-th]].
- [11] A. Kievsky, M. Viviani, D. Logoteta, I. Bombaci and L. Girlanda, Phys. Rev. Lett. **121** (2018), no. 7, 072701 doi:[10.1103/PhysRevLett.121.072701](https://doi.org/10.1103/PhysRevLett.121.072701) [[arXiv:1806.02636](#) [nucl-th]].
- [12] I. Tews, J. M. Lattimer, A. Ohnishi and E. E. Kolomeitsev, Astrophys. J. **848** (2017), no. 2, 105 doi:[10.3847/1538-4357/aa8db9](https://doi.org/10.3847/1538-4357/aa8db9) [[arXiv:1611.07133](#) [nucl-th]].
- [13] M. Gattobigio, A. Kievsky and M. Viviani, Phys. Rev. C **100** (2019), no. 3, 034004 doi:[10.1103/PhysRevC.100.034004](https://doi.org/10.1103/PhysRevC.100.034004) [[arXiv:1903.08900](#) [nucl-th]].
- [14] A. Kievsky, A. Polls, B. Juliá-Díaz, N. K. Timofeyuk and M. Gattobigio, Phys. Rev. A **102** (2020), no. 6, 063320 doi:[10.1103/PhysRevA.102.063320](https://doi.org/10.1103/PhysRevA.102.063320) [[arXiv:2006.09758](#) [cond-mat.quant-gas]].
- [15] P. E. Georgoudis, Nucl. Phys. A **1015** (2021), 122297 doi:[10.1016/j.nuclphysa.2021.122297](https://doi.org/10.1016/j.nuclphysa.2021.122297) [[arXiv:2006.15508](#) [nucl-th]].
- [16] P. E. Georgoudis, Adv. Nucl. Phys. **28** (2022), 167-172 doi:[10.12681/hnps.3600](https://doi.org/10.12681/hnps.3600)

- [17] L. Contessi, J. Kirscher and M. Pavon Valderrama, Phys. Rev. A **109** (2024) no.3, 032217 doi:[10.1103/PhysRevA.109.032217](https://doi.org/10.1103/PhysRevA.109.032217) [[arXiv:2303.01312](https://arxiv.org/abs/2303.01312) [cond-mat.quant-gas]].
- [18] U. van Kolck, Eur. Phys. J. A **56** (2020), no. 3, 97 doi:[10.1140/epja/s10050-020-00092-1](https://doi.org/10.1140/epja/s10050-020-00092-1) [[arXiv:2003.09974](https://arxiv.org/abs/2003.09974) [nucl-th]].
- [19] A. Kievsky, L. Girlanda, M. Gattobigio and M. Viviani, Ann. Rev. Nucl. Part. Sci. **71** (2021), 465-490 doi:[10.1146/annurev-nucl-102419-032845](https://doi.org/10.1146/annurev-nucl-102419-032845) [[arXiv:2102.13504](https://arxiv.org/abs/2102.13504) [nucl-th]].
- [20] V. G. J. Stoks, R. A. M. Klomp, M. C. M. Rentmeester and J. J. de Swart, Phys. Rev. C **48** (1993), 792-815 doi:[10.1103/PhysRevC.48.792](https://doi.org/10.1103/PhysRevC.48.792), nn-online.org accessed August 2024.
- [21] R. Navarro Pérez, J. E. Amaro and E. Ruiz Arriola, Phys. Rev. C **88** (2013), 024002 [erratum: Phys. Rev. C **88** (2013), no. 6, 069902] doi:[10.1103/PhysRevC.88.024002](https://doi.org/10.1103/PhysRevC.88.024002) [[arXiv:1304.0895](https://arxiv.org/abs/1304.0895) [nucl-th]].
- [22] R. Navarro Pérez, J. E. Amaro and E. Ruiz Arriola, Phys. Rev. C **88** (2013), no. 6, 064002 [erratum: Phys. Rev. C **91** (2015), no. 2, 029901] doi:[10.1103/PhysRevC.88.064002](https://doi.org/10.1103/PhysRevC.88.064002) [[arXiv:1310.2536](https://arxiv.org/abs/1310.2536) [nucl-th]].
- [23] E. Ruiz Arriola, J. E. Amaro and R. Navarro Pérez, Front. in Phys. **8** (2020), 1 doi:[10.3389/fphy.2020.00001](https://doi.org/10.3389/fphy.2020.00001) [[arXiv:1911.09637](https://arxiv.org/abs/1911.09637) [nucl-th]].
- [24] N. Kaiser, R. Brockmann and W. Weise, Nucl. Phys. A **625** (1997), 758-788 doi:[10.1016/S0375-9474\(97\)00586-1](https://doi.org/10.1016/S0375-9474(97)00586-1) [[arXiv:nuc1-th/9706045](https://arxiv.org/abs/nuc1-th/9706045) [nucl-th]].
- [25] S. R. Beane, P. F. Bedaque, M. J. Savage and U. van Kolck, Nucl. Phys. A **700** (2002), 377-402 doi:[10.1016/S0375-9474\(01\)01324-0](https://doi.org/10.1016/S0375-9474(01)01324-0) [[arXiv:nuc1-th/0104030](https://arxiv.org/abs/nuc1-th/0104030) [nucl-th]].
- [26] M. C. Birse, Phys. Rev. C **74** (2006), 014003 doi:[10.1103/PhysRevC.74.014003](https://doi.org/10.1103/PhysRevC.74.014003) [[nucl-th/0507077](https://arxiv.org/abs/nuc1-th/0507077)].
- [27] M. C. Birse, PoS CD **09** (2009), 078 doi:[10.22323/1.086.0078](https://doi.org/10.22323/1.086.0078) [[arXiv:0909.4641](https://arxiv.org/abs/0909.4641) [nucl-th]].
- [28] E. Wigner, Phys. Rev. **51** (1937), 106; *ibid.* **56** (1939), 519.
- [29] F. Hund, Zeitschrift für Physik **105** (1937) 202.
- [30] T. Mehen, I. W. Stewart and M. B. Wise, Phys. Rev. Lett. **83** (1999), 931-934 doi:[10.1103/PhysRevLett.83.931](https://doi.org/10.1103/PhysRevLett.83.931) [[arXiv:hep-ph/9902370](https://arxiv.org/abs/hep-ph/9902370) [hep-ph]].
- [31] E. Epelbaum, U. G. Meissner, W. Gloeckle and C. Elster, Phys. Rev. C **65** (2002), 044001 doi:[10.1103/PhysRevC.65.044001](https://doi.org/10.1103/PhysRevC.65.044001) [[arXiv:nuc1-th/0106007](https://arxiv.org/abs/nuc1-th/0106007) [nucl-th]].
- [32] D. O. Riska, Nucl. Phys. A **710** (2002), 55-82 doi:[10.1016/S0375-9474\(02\)01091-6](https://doi.org/10.1016/S0375-9474(02)01091-6) [[arXiv:nuc1-th/0204016](https://arxiv.org/abs/nuc1-th/0204016) [nucl-th]].

- [33] D. B. Kaplan and M. J. Savage, Phys. Lett. B **365** (1996), 244-251 doi:[10.1016/0370-2693\(95\)01277-X](#) [[arXiv:hep-ph/9509371](#) [hep-ph]].
- [34] D. B. Kaplan and A. V. Manohar, Phys. Rev. C **56** (1997), 76-83 doi:[10.1103/PhysRevC.56.76](#) [[arXiv:nucl-th/9612021](#) [nucl-th]].
- [35] A. Calle Cordón and E. Ruiz Arriola, Phys. Rev. C **78** (2008), 054002 doi:[10.1103/PhysRevC.78.054002](#) [[arXiv:0807.2918](#) [nucl-th]].
- [36] E. Ruiz Arriola, Symmetry **8** (2016) no.6, 42 doi:[10.3390/sym8060042](#)
- [37] E. Noether, Nachrichten von der Gesellschaft der Wissenschaften zu Göttingen, Mathematisch-Physikalische Klasse 1918 (1918), 235, online at [eudml.org/doc/59024](#).
- [38] M. C. Birse, J. A. McGovern and K. G. Richardson, Phys. Lett. B **464** (1999), 169-176 doi:[10.1016/S0370-2693\(99\)00991-0](#) [[arXiv:hep-ph/9807302](#) [hep-ph]].
- [39] T. Barford and M. C. Birse, Phys. Rev. C **67** (2003), 064006 doi:[10.1103/PhysRevC.67.064006](#) [[arXiv:hep-ph/0206146](#) [hep-ph]].
- [40] P. F. Bedaque, H. W. Hammer and U. van Kolck, Nucl. Phys. A **676** (2000), 357-370 doi:[10.1016/S0375-9474\(00\)00205-0](#) [[arXiv:nucl-th/9906032](#) [nucl-th]].
- [41] H. W. Griesshammer and M. R. Schindler, Eur. Phys. J. A **46** (2010), 73-83 doi:[10.1140/epja/i2010-11017-x](#) [[arXiv:1007.0734](#) [nucl-th]].
- [42] J. Vanasse, Phys. Rev. C **86** (2012), 014001 doi:[10.1103/PhysRevC.86.014001](#) [[arXiv:1110.1039](#) [nucl-th]].
- [43] X. Lin, H. Singh, R. P. Springer and J. Vanasse, Phys. Rev. C **108** (2023), no. 4, 044001 doi:[10.1103/PhysRevC.108.044001](#) [[arXiv:2210.15650](#) [nucl-th]].
- [44] X. Lin and J. Vanasse, [[arXiv:2408.14602](#) [nucl-th]].
- [45] B. N. Lu, N. Li, S. Elhatisari, D. Lee, E. Epelbaum and U. G. Meißner, Phys. Lett. B **797** (2019), 134863 doi:[10.1016/j.physletb.2019.134863](#) [[arXiv:1812.10928](#) [nucl-th]].
- [46] D. Lee, S. Bogner, B. A. Brown, S. Elhatisari, E. Epelbaum, H. Hergert, M. Hjorth-Jensen, H. Krebs, N. Li and B. N. Lu, *et al.* Phys. Rev. Lett. **127** (2021), no. 6, 062501 doi:[10.1103/PhysRevLett.127.062501](#) [[arXiv:2010.09420](#) [nucl-th]].
- [47] I. N. Izosimov, doi:[10.1142/9789811209451_0009](#)
- [48] S. Shen, T. A. Lähde, D. Lee and U. G. Meißner, Eur. Phys. J. A **57** (2021), no. 9, 276 doi:[10.1140/epja/s10050-021-00586-6](#) [[arXiv:2106.04834](#) [nucl-th]].
- [49] A. Ekström and L. Platter, [[arXiv:2409.08197](#) [nucl-th]].

- [50] H. W. Griebhammer, S. König, D. R. Phillips, U. van Kolck, in: *Nuclear Forces for Precision Nuclear Physics – a collection of perspectives*, I. Tews, Z. Davoudi, A. Ekström, J. D. Holt (eds.), Few-Body Syst. **63** (2022) 67 doi:[10.1007/s00601-022-01749-x](https://doi.org/10.1007/s00601-022-01749-x) [[arXiv:2202.01105](https://arxiv.org/abs/2202.01105) [nucl-th]].
- [51] D. B. Kaplan, M. J. Savage and M. B. Wise, Phys. Lett. B **424** (1998), 390-396 doi:[10.1016/S0370-2693\(98\)00210-X](https://doi.org/10.1016/S0370-2693(98)00210-X) [[arXiv:nucl-th/9801034](https://arxiv.org/abs/nucl-th/9801034) [nucl-th]].
- [52] D. B. Kaplan, M. J. Savage and M. B. Wise, Nucl. Phys. B **534** (1998), 329-355 doi:[10.1016/S0550-3213\(98\)00440-4](https://doi.org/10.1016/S0550-3213(98)00440-4) [[arXiv:nucl-th/9802075](https://arxiv.org/abs/nucl-th/9802075) [nucl-th]].
- [53] S. Fleming, T. Mehen and I. W. Stewart, Nucl. Phys. A **677** (2000), 313-366 doi:[10.1016/S0375-9474\(00\)00221-9](https://doi.org/10.1016/S0375-9474(00)00221-9) [[arXiv:nucl-th/9911001](https://arxiv.org/abs/nucl-th/9911001) [nucl-th]].
- [54] S. Fleming, T. Mehen and I. W. Stewart, Phys. Rev. C **61** (2000), 044005 doi:[10.1103/PhysRevC.61.044005](https://doi.org/10.1103/PhysRevC.61.044005) [[arXiv:nucl-th/9906056](https://arxiv.org/abs/nucl-th/9906056) [nucl-th]].
- [55] F. Oosterhof, B. Long, J. de Vries, R. G. E. Timmermans and U. van Kolck, Phys. Rev. Lett. **122** (2019) no.17, 172501 doi:[10.1103/PhysRevLett.122.172501](https://doi.org/10.1103/PhysRevLett.122.172501) [[arXiv:1902.05342](https://arxiv.org/abs/1902.05342) [hep-ph]].
- [56] F. Oosterhof, J. de Vries, R. G. E. Timmermans and U. van Kolck, Phys. Lett. B **820** (2021), 136525 doi:[10.1016/j.physletb.2021.136525](https://doi.org/10.1016/j.physletb.2021.136525) [[arXiv:2105.05715](https://arxiv.org/abs/2105.05715) [nucl-th]].
- [57] F. Oosterhof, *Baryon-Number Violation in Chiral Effective Field Theory*, PhD thesis, University of Groningen 2022.
- [58] S. R. Beane, D. B. Kaplan and A. Vuorinen, Phys. Rev. C **80** (2009), 011001 doi:[10.1103/PhysRevC.80.011001](https://doi.org/10.1103/PhysRevC.80.011001) [[arXiv:0812.3938](https://arxiv.org/abs/0812.3938) [nucl-th]].
- [59] D. B. Kaplan, Phys. Rev. C **102** (2020) no. 3, 034004 doi:[10.1103/PhysRevC.102.034004](https://doi.org/10.1103/PhysRevC.102.034004) [[arXiv:1905.07485](https://arxiv.org/abs/1905.07485) [nucl-th]].
- [60] H. W. Griebhammer, Eur. Phys. J. A **56** (2020), no. 4, 118 doi:[10.1140/epja/s10050-020-00129-5](https://doi.org/10.1140/epja/s10050-020-00129-5) [[arXiv:2004.00411](https://arxiv.org/abs/2004.00411) [nucl-th]].
- [61] H. W. Griebhammer, Few Body Syst. **63** (2022), no. 2, 44 doi:[10.1007/s00601-022-01739-z](https://doi.org/10.1007/s00601-022-01739-z) [[arXiv:2111.00930](https://arxiv.org/abs/2111.00930) [nucl-th]].
- [62] G. Rupak and N. Shores, Phys. Rev. C **60** (1999), 054004 doi:[10.1103/PhysRevC.60.054004](https://doi.org/10.1103/PhysRevC.60.054004) [[arXiv:nucl-th/9902077](https://arxiv.org/abs/nucl-th/9902077) [nucl-th]].
- [63] Y. P. Teng, *The Unitarity Limit of NN Scattering With Perturbative Pions to N²LO*, MS thesis, George Washington University 2023.
- [64] H. W. Griebhammer, *What Can Possibly Go Wrong?*, ECT* workshop THE NUCLEAR INTERACTION: POST-MODERN DEVELOPMENTS, Trento (Italy), 19 August 2024.

- [65] H. W. Griedhammer, *The Unitarity Limit of the NN System with Perturbative Pions*, CHIRAL DYNAMICS 2024, Bochum (Germany), 26 August 2024.
- [66] H. W. Griedhammer, *Two Nucleons Near Unitarity with Perturbative Pions: Persistence vs Chiral Symmetry*, INT-24-3 QUANTUM FEW- AND MANY-BODY SYSTEMS IN UNIVERSAL REGIMES, Seattle (USA), 17 October 2024.
- [67] J. Schwinger, hectographed notes on nuclear physics, Harvard University 1947.
- [68] G. F. Chew and M. L. Goldberger, Phys. Rev. **75** (1949) 1637.
- [69] F. C. Barker and R. E. Peierls, Phys. Rev. **75** (1949), 3122.
- [70] H. A. Bethe, Phys. Rev. **76** (1949), 38.
- [71] R. Bellman, *Perturbation Techniques in Mathematics, Physics and Engineering*, Holt, Rinehart and Winston 1964.
- [72] C. M. Bender and S. A. Orszag, *Advanced Mathematical Methods for Scientists and Engineers*, McGraw Hill 1978.
- [73] J. A. Murdock, *Perturbations – Theory and Methods*, John Wiley & Sons 1991.
- [74] M. H. Holmes, *Introduction to Perturbation Methods*, 2nd ed., Springer 2013.
- [75] H. P. Stapp, T. J. Ypsilantis, and N. Metropolis, Phys. Rev. **105** (1957), 302.
- [76] P. F. Bedaque and H. W. Griedhammer, Nucl. Phys. A **671** (2000), 357-379 doi:[10.1016/S0375-9474\(99\)00691-0](https://doi.org/10.1016/S0375-9474(99)00691-0) [[arXiv:nuc1-th/9907077](https://arxiv.org/abs/nuc1-th/9907077) [[nucl-th](#)]].
- [77] H. W. Griedhammer, *Technical Note: Strict Perturbation Theory for Nonperturbative Algorithms*, distributed in response to the ECT* workshop NEW IDEAS IN CONSTRAINING NUCLEAR FORCES 2018, updated April 2021, available from the author.
- [78] H. W. Griedhammer, J. A. McGovern, D. R. Phillips and G. Feldman, Prog. Part. Nucl. Phys. **67** (2012), 841-897 doi:[10.1016/j.ppnp.2012.04.003](https://doi.org/10.1016/j.ppnp.2012.04.003) [[arXiv:1203.6834](https://arxiv.org/abs/1203.6834) [[nucl-th](#)]].
- [79] M. Cacciari and N. Houdeau, JHEP **1109** (2011), 039 [[arXiv:1105.5152](https://arxiv.org/abs/1105.5152) [[hep-ph](#)]].
- [80] R. J. Furnstahl, N. Klco, D. R. Phillips and S. Wesolowski, Phys. Rev. C **92** (2015), 024005 [[arXiv:1506.01343](https://arxiv.org/abs/1506.01343) [[nucl-th](#)]].
- [81] H. W. Griedhammer, J. A. McGovern and D. R. Phillips, Eur. Phys. J. A **52** (2016), no. 5, 139 doi:[10.1140/epja/i2016-16139-5](https://doi.org/10.1140/epja/i2016-16139-5) [[arXiv:1511.01952](https://arxiv.org/abs/1511.01952) [[nucl-th](#)]].
- [82] H. W. Griedhammer, Nucl. Phys. A **744** (2004), 192-226 doi:[10.1016/j.nuclphysa.2004.08.012](https://doi.org/10.1016/j.nuclphysa.2004.08.012) [[arXiv:nuc1-th/0404073](https://arxiv.org/abs/nuc1-th/0404073) [[nucl-th](#)]].

- [83] Y. P. Teng and H. W. Griesshammer, *The Unitarity Expansion in χ EFT with Perturbative Pions in the Mixed $^3\text{SD}_1$ and Higher NN Partial Waves*, in preparation.
- [84] D. B. Kaplan, M. J. Savage and M. B. Wise, Phys. Rev. C **59** (1999), 617-629 doi:[10.1103/PhysRevC.59.617](#) [[arXiv:nucl-th/9804032](#) [nucl-th]].
- [85] J. J. de Swart, C. P. F. Terheggen and V. G. J. Stoks, [[arXiv:nucl-th/9509032](#) [nucl-th]].
- [86] F. W. Olver, D. W. Lozier, R. Boisvert and C. W. Clark (eds.), *The NIST Handbook of Mathematical Functions*, Cambridge University Press 2010.
- [87] T. D. Cohen and J. M. Hansen, Phys. Rev. C **59** (1999), 13-20 doi:[10.1103/PhysRevC.59.13](#) [[arXiv:nucl-th/9808038](#) [nucl-th]].
- [88] T. D. Cohen and J. M. Hansen, Phys. Rev. C **59** (1999), 3047-3051 doi:[10.1103/PhysRevC.59.3047](#) [[arXiv:nucl-th/9901065](#) [nucl-th]].
- [89] T. D. Cohen and J. M. Hansen, [[arXiv:nucl-th/9908049](#) [nucl-th]].
- [90] O. Thim, Few Body Syst. **65** (2024), no. 3, 69 doi:[10.1007/s00601-024-01938-w](#) [[arXiv:2403.10292](#) [nucl-th]].
- [91] H. W. Griesshammer, PoS **CD15** (2016), 104 doi:[10.22323/1.253.0104](#) [[arXiv:1511.00490](#) [nucl-th]].
- [92] G. 't Hooft, NATO Sci. Ser. B **59** (1980), 135 doi:[10.1007/978-1-4684-7571-5_9](#).
- [93] A. Manohar and H. Georgi, Nucl. Phys. B **234** (1984), 189 [n.b. Acknowledgement] doi:[10.1016/0550-3213\(84\)90231-1](#).
- [94] H. Georgi and L. Randall, Nucl. Phys. B **276** (1986), 241 doi:[10.1016/0550-3213\(86\)90022-2](#).
- [95] S. Weinberg, Phys. Rev. Lett. **63** (1989), 2333 doi:[10.1103/PhysRevLett.63.2333](#).
- [96] H. Georgi, Phys. Lett. B **298** (1993), 187 doi:[10.1016/0370-2693\(93\)91728-6](#) [[hep-ph/9207278](#)].
- [97] H. W. Griesshammer, Nucl. Phys. A **760** (2005), 110 doi:[10.1016/j.nuclphysa.2005.05.202](#) [[nucl-th/0502039](#)].
- [98] U. van Kolck, *Tower of Effective Field Theories: Status and Perspectives*, workshop THE TOWER OF EFFECTIVE (FIELD), THEORIES AND THE EMERGENCE OF NUCLEAR PHENOMENA , CEA/SPhN Saclay (France), 17 January 2017.
- [99] R. Landau, J. Páez and C. Bordeianu, *A Survey of Computational Physics: Introductory Computational Science*, Princeton University Press 2008.
- [100] G. P. Lepage, [[nucl-th/9706029](#)].

- [101] *Enhancing the Interaction between Nuclear Experiment and Theory Through Information and Statistics*, **special issue J. Phys. G** **42** (2015), no. 3.
- [102] *Further Enhancing the Interaction between Nuclear Experiment and Theory through Information and Statistics (ISNET 2.0)*, **special issue J. Phys. G** **46** (2019), no. 10.
- [103] D. R. Phillips, R. J. Furnstahl, U. Heinz, T. Maiti, W. Nazarewicz, F. M. Nunes, M. Plumlee, M. T. Pratola, S. Pratt and F. G. Viens, *et al.* J. Phys. G **48** (2021), no. 7, 072001 doi:[10.1088/1361-6471/abf1df](https://doi.org/10.1088/1361-6471/abf1df) [[arXiv:2012.07704](https://arxiv.org/abs/2012.07704) [nucl-th]].
- [104] J. W. Chen, H. W. Griesshammer, M. J. Savage and R. P. Springer, Nucl. Phys. A **644** (1998), 221-234 doi:[10.1016/S0375-9474\(98\)80012-2](https://doi.org/10.1016/S0375-9474(98)80012-2) [[arXiv:nucl-th/9806080](https://arxiv.org/abs/nucl-th/9806080) [nucl-th]].
- [105] J. W. Chen, H. W. Griesshammer, M. J. Savage and R. P. Springer, Nucl. Phys. A **644** (1998), 245-259 doi:[10.1016/S0375-9474\(98\)00591-0](https://doi.org/10.1016/S0375-9474(98)00591-0) [[arXiv:nucl-th/9809023](https://arxiv.org/abs/nucl-th/9809023) [nucl-th]].
- [106] M. J. Savage and R. P. Springer, Nucl. Phys. A **686** (2001), 413-428 doi:[10.1016/S0375-9474\(00\)00568-6](https://doi.org/10.1016/S0375-9474(00)00568-6) [[arXiv:nucl-th/9907069](https://arxiv.org/abs/nucl-th/9907069) [nucl-th]].
- [107] B. Borasoy and H. W. Griesshammer, Int. J. Mod. Phys. E **12** (2003), 65-80 doi:[10.1142/S0218301303001156](https://doi.org/10.1142/S0218301303001156) [[arXiv:nucl-th/0105048](https://arxiv.org/abs/nucl-th/0105048) [nucl-th]].
- [108] H. W. Griesshammer, *Unitarity for Two Nucleons with Pions*, 2019 FALL MEETING OF THE DIVISION OF NUCLEAR PHYSICS OF THE AMERICAN PHYSICAL SOCIETY, Washington DC (USA), 15 October 2019.
- [109] H. W. Griesshammer, *Are Nucleon-Nucleon Interactions As Important As We Think?*, MAIER-LEIBNITZ-COLLOQUIUM, Physics Departments of TU München and München University, 8 July 2021.
- [110] H. W. Griesshammer, in preparation.